From the holdings of the Department of Special Collections , Princeton University Library, Princeton, NJ

These documents are either in the public domain, or can only be used for educational and research purposes (Fair use) as per U.S. Copyright law (text below). By accessing this file, all users agree that their use falls in the public domain or within fair use as defined by the copyrightlaw. We do not charge any permission or usage fees for the publication of images of material inour collections, including those provided by Princeton University Library, via our website, catalog, or directly from staff.For more information regarding copyright, credit, and citation please review the information onthe Copyright, Credit and Citation Guidelines page of our website.
https://library.princeton.edu/special-collections/policies/copyright-credit-and-citation-guidelines. If you have any questions, including how to order higher-quality images from the collection, contact Special Collections Public Services via our Ask Us! Form. https://library.princeton.edu/special-collections/ask-us

---

Doctoral Dissertations, 2011-2026 Mathematics

2016

Applications of Heegaard Floer Homology to Knot Concordance

Truong, Linh My

Princeton, NJ : Princeton University

---

http://arks.princeton.edu/ark:/88435/dsp019880vt394

U.S. Copyright law: The copyright law of the United States (Title 17, §108, United States Code) governs the making of photocopies or other reproductions of copyrighted material. Under certain conditions specified in the law, libraries and archives are authorized to furnish a photocopy or other reproduction. One of these specified conditions is that the photocopy or reproduction is not to be used for any purpose other than private study, scholarship, or research. If a user makes a request for, or later uses, a photocopy or reproduction for purposes in excess of fair use that user may be liable for copyright infringement. This institution reserves the right to refuse to accept a copying order if, in its judgment, fulfillment of the order would involve a violation of copyright law. https://www.copyright.gov/title17/title17.pdf

Applications of Heegaard Floer Homology to Knot Concordance

Linh My Truong

A Dissertation
Presented to the Faculty
of Princeton University
in Candidacy for the Degree
of Doctor of Philosophy

Recommended for Acceptance
by the Department of
Mathematics
Adviser: Peter Ozsváth
Adviser: Zoltán Szabó

May 2016

© Copyright by Linh My Truong, 2016.

All rights reserved.

Abstract

We consider several applications of Heegaard Floer homology to the study of knot concordance.

Using the techniques of bordered Heegaard Floer homology, we compute the concordance invariant τ for a family of satellite knots that generalizes Whitehead doubles.

We also construct an integer lift $\tilde{\epsilon}$ of the concordance invariant ϵ. We introduce an interpretation of $\tilde{\epsilon}$ in terms of a filtration on $\widehat{\mathrm{CF}}(S^3_N K)$ induced by a family of knots $\mu_n \subset S^3_N K$.

Finally, we use truncated Heegaard Floer homology to construct a sequence of concordance invariants ν_n that generalizes previously known concordance invariants ν, ν', and ν^+.

Acknowledgements

First of all, I would like to thank my advisors, Peter Ozsváth and Zoltán Szabó, for all of their guidance throughout my time as a graduate student.

I thank Jen Hom, Chuck Livingston, and Adam Levine for helpful conversations and for their interest in my work. Furthermore, I would like to thank Adam Levine for detailed comments and corrections on a draft of this thesis.

I have benefitted from many discussions with other topology graduate students – Chris Yang Xiu, Nate Dowlin, Mike Wong, Bohua Zhan, Andy Manion, Béla Rácz, Cotton Seed, and Sam Lewallen, among others. I thank them for enriching my graduate school experience.

I am grateful to my parents and family for their love and support.

Finally, I thank my husband Alex for his constant support, love and the immeasurable joy that he brings to my life.

To my mother, Ba Truong.

Contents

Abstract . . . iii

Acknowledgements . . . iv

1 Introduction **1**

1.1 Summary of Results . . . 1

1.2 Organization of the thesis . . . 3

2 Background on Heegaard Floer Homology and Knot Concordance **4**

2.1 Heegaard diagrams and symmetric products . . . 4

2.2 Heegaard Floer homology . . . 6

2.2.1 $\widehat{\mathrm{HF}}(Y,\mathfrak{t})$ . . . 7

2.2.2 $\mathrm{HF}^{\infty}(Y,t)$ . . . 8

2.2.3 $\mathrm{HF}^{+}(Y,\mathfrak{t})$ and $\mathrm{HF}^{-}(Y,\mathfrak{t})$ . . . 8

2.3 Knot Floer homology . . . 9

2.3.1 $\widehat{\mathrm{HFK}}(K)$ . . . 9

2.3.2 HFK^{-} and HFK^{+} . . . 10

2.3.3 CFK^{∞} . . . 11

2.4 Concordance invariants and Heegaard Floer homology . . . 11

2.4.1 Cobordism maps on $\widehat{\mathrm{HF}}$ . . . 12

2.4.2 The Ozsváth-Szabó τ invariant . . . 13

2.4.3 The concordance invariants ν and ν' . . . 14

2.4.4 Cobordism maps on HF^{+} . . . 14

2.4.5 The Hom-Wu ν^{+} invariant . . . 15

2.4.6 The concordance invariant $\nu^{+'}$ . . . 16

3 Bordered Floer Homology and Generalized Whitehead Doubles **17**

3.1 Background on Bordered Floer Homology for three-manifolds with torus boundary 17

3.2 Bordered Floer Homology and Whitehead Doubles 20

3.3 Generalized Whitehead Doubles 23

3.4 Further Directions 30

4 Knot Floer Homology of a Family of Knots μ_n in $S^3_t K$, $t >> 0$, and Concordance Invariants **31**

4.1 Knot Floer Homology of a Family of Knots μ_n in $S^3_t K$, $t >> 0$, in terms of $\mathrm{CFK}^\infty(S^3, K)$ . . 31

4.2 Background on the concordance invariants ϵ and a_1 34

4.3 A refinement of ϵ 36

4.4 Further Directions 41

4.4.1 Properties of $\tilde{\epsilon}$ 41

4.4.2 Construct an HF^+ version of ϵ and $\tilde{\epsilon}$ 41

4.4.3 Generalizing the two-component link used in the construction of $\tilde{\epsilon}$ 41

5 Truncated Heegaard Floer Homology and Concordance Invariants **42**

5.1 Truncated Heegaard Floer homology 43

5.2 A sequence of concordance invariants ν_n 44

Bibliography **50**

Chapter 1

Introduction

1.1 Summary of Results

This thesis consists of three main parts, contained in Chapters 3, 4, and 5, and we summarize the results in this section.

In Chapter 3 we introduce a family of satellite knots $W(K,t;n)$ indexed by two parameters, t, the twisting coefficient, and n, the number of full twists in the clasp region. The satellite knot $W(K,t;1)$ (resp. $W(K,t;-1)$) is the ordinary Whitehead double $D_+(K,t)$ (resp. $D_-(K,t)$) of K. We call these knots t-twisted n-clasped generalized Whitehead doubles. Generalized Whitehead doubles are a special case of a family of knots that Levine [15] previously studied, and the results presented in Chapter 3 agree with his work. This work is independent of Levine. We use techniques in bordered Floer homology to compute τ of generalized Whitehead doubles in terms of τ of the companion knot. The main result is the computation of $\tau(W(K,t;n))$:

Theorem 1.1.1. *Let $W(K,t;n)$ be the t-twisted, n-clasped generalized Whitehead double of K.*

$$\tau(W(K,t;n)) = \begin{cases} -1, & \text{if } t > 2\tau(K) \text{ and } n < 0; \\ 1, & \text{if } t < 2\tau(K) \text{ and } n > 0; \\ 0, & \text{otherwise.} \end{cases}$$

In Chapter 4 we construct an integer lift $\tilde{\epsilon}$ of the Hom concordance invariant ϵ and give an interpretation of this invariant in terms of filtered cobordism maps.

Definition 1.1.2. Given a knot K inside S^3, let $C = \mathrm{CFK}^\infty$ and consider the maps

$$G_{-n,\tau} : C\{\max(i, j-\tau) = 0, i \geq -n\} \to C\{i = 0\}$$
$$F_{n,\tau} : C\{i = 0\} \to C\{\min(i, j-\tau) = 0, i \leq n\}.$$

Define the integer-valued knot invariant $\tilde{\epsilon}(K)$ as follows:

$$\tilde{\epsilon}(K) = \begin{cases} \max\{-n \mid G_{-n,\tau} \text{ is trivial on homology}\}\,, & \text{if } \epsilon(K) = -1; \\ 0, & \text{if } \epsilon(K) = 0; \\ \min\{n \mid F_{n,\tau} \text{ is trivial on homology}\}\,, & \text{if } \epsilon(K) = 1. \end{cases}$$

Proposition 1.1.3. *The invariant $\tilde{\epsilon}$ satisfies the following properties:*

(1) If K is smoothly slice, then $\tilde{\epsilon}(K) = 0$.

(2) $\mathrm{sgn}(\tilde{\epsilon}(K)) = \mathrm{sgn}(\epsilon(K))$.

(3) $\tilde{\epsilon}(K) = -\tilde{\epsilon}(\overline{K})$.

(4) If $\tilde{\epsilon}(K) = 0$, then $\tilde{\epsilon}(K\#K') = \tilde{\epsilon}(K')$.

These properties imply that $\tilde{\epsilon}$ is a concordance invariant.

One of the main results of Chapter 4 is a reformulation of the invariant $\tilde{\epsilon}$, in terms of *filtered* cobordism maps associated to large integer surgery along K and a knot μ_n inside $S^3_N K$.

Theorem 1.1.4. *Let $\mu_n \subset S^3_N K$ be a knot that is homologically equivalent to $n \cdot \mu$, or n times the meridian of K, inside $S^3_N K$ where N is sufficiently large. An alternative definition of $\tilde{\epsilon}(K)$ is the following:* $\tilde{\epsilon}(K) =$

$$\begin{cases} \max\left\{m \mid \frac{\widehat{\mathrm{CFK}}(S^3_N K, \mathfrak{s}_\tau, \mu_n)}{\mathcal{F}(\mu_n, top-1-m)} \to \widehat{\mathrm{CF}}(S^3) \text{ is trivial on } H_*\right\}, & \text{if } \epsilon(K) = -1; \\ 0, & \text{if } \epsilon(K) = 0; \\ \min\left\{m \mid \widehat{\mathrm{CF}}(S^3) \to \mathcal{F}'(\mu_n, bottom + m) \subset \widehat{\mathrm{CFK}}(S^3_{-N} K, \mathfrak{s}_\tau, \mu_n) \text{ is trivial on } H_*\right\}, & \text{if } \epsilon(K) = 1; \end{cases}$$

where n, N are sufficiently large, $\mathcal{F}(\mu_n, top - m)$ denotes the filtered subcomplex of $\widehat{\mathrm{CFK}}(S^3_N K, \mathfrak{s}_\tau, \mu_n)$ consisting of generators with Alexander filtration $\leq top - m$, top is the highest Alexander filtration level of $\widehat{\mathrm{CFK}}(S^3_N K, \mathfrak{s}_\tau, \mu_n)$, $\mathcal{F}'(\mu_n, bottom + m) \subset \widehat{\mathrm{CFK}}(S^3_{-N} K, \mathfrak{s}_\tau, \mu_n)$ denotes the subcomplex consisting of generators with Alexander filtration $\leq bottom + m$, and bottom is the lowest Alexander filtration level of $\widehat{\mathrm{CFK}}(S^3_{-N} K, \mathfrak{s}_\tau, \mu_n)$.

In Chapter 5 we use truncated Heegaard Floer homology to construct a sequence of concordance invariants ν_n that generalizes previously known concordance invariants ν, ν', and ν^+. The invariants ν_n satisfy the following properties:

- $\nu_n(K)$ is a concordance invariant.
- $\nu_1(K) = \nu(K)$ and $\nu_{-1}(K) = \nu'(K)$.
- $\nu_n(K) \leq \nu_{n+1}(K)$.
- For sufficiently large positive n, $\nu_n(K) = \nu^+(K)$.
- For sufficiently large negative n, $\nu_n(K) = \nu^{+'}(K)$.

1.2 Organization of the thesis

In Chapter 2, we present background on Heegaard Floer homology, knot Floer homology, knot concordance, and concordance invariants. In Chapter 3, we study generalized Whitehead doubles using bordered Floer homology and compute τ for this family of satellite knots. In Chapter 4, we discuss the refinement $\tilde{\epsilon}$ of Hom's ϵ and its reformulation in terms of filtered cobordism maps. In Chapter 5, we introduce the sequence of concordance invariants ν_n and discuss its properties.

Chapter 2

Background on Heegaard Floer Homology and Knot Concordance

Heegaard Floer homology, defined by Ozsváth and Szabó in [25], is an invariant for closed three-manifolds defined using Heegaard diagrams and symplectic geometry. Heegaard Floer invariants have led to a wealth of topological results: detection of the Seifert genus of knots; detection of fiberedness for knots and three-manifolds; bounds on the unknotting number and slice genus; and more. It is known to be equivalent to several other gauge-theoretic or holomorphic curve invariants including monopole Floer homology [14] and embedded contact homology [2]. The theory has been extended to knots [23], [31], three-manifolds with one- or two-component boundary [16], and four-dimensional cobordisms between three-manifolds [26].

2.1 Heegaard diagrams and symmetric products

Let Y be a closed, oriented smooth three-manifold. We describe decompositions of Y into simpler pieces called *handlebodies*.

A *genus g handlebody* U is a regular neighborhood of a wedge of g circles in $\mathbb{R}^3$. The boundary of U is an oriented genus g surface, denoted Σ_g or Σ. If we glue two genus g handlebodies U_0 and U_1 along their boundary $\partial U_0 = -\partial U_1 = \Sigma$, we get a closed oriented three-manifold

$$Y = U_0 \cup_\Sigma U_1,$$

and this is called a *Heegaard decomposition* for Y.

Definition 2.1.1. A *set of attaching circles* $\{\gamma_1, \ldots, \gamma_g\}$ for a genus g handlebody U is a collection of curves embedded in $\partial U = \Sigma_g$ satisfying the following conditions:

1. The curves γ_i are mutually disjoint.
2. $\Sigma_g - \gamma_1 - \cdots - \gamma_g$ is connected. Equivalently, $\{[\gamma_1], \ldots, [\gamma_g]\}$ is linearly independent in $H_1(\Sigma_g; \mathbb{Z})$.
3. The curves γ_i bound embedded disks in U.

Definition 2.1.2. Let $Y = U_0 \cup_{\Sigma_g} U_1$ be a Heegaard decomposition. A compatible *(pointed) Heegaard diagram* for Y consists of $(\Sigma_g, \alpha_1, \ldots, \alpha_g, \beta_1, \ldots, \beta_g, z)$, where $\{\alpha_1, \ldots, \alpha_g\}$ is a set of attaching circles for U_0, $\{\beta_1, \ldots, \beta_g\}$ is a set of attaching circles for U_1, and $z \in \Sigma - \alpha_1 - \cdots - \alpha_g - \beta_1 - \cdots - \beta_g$ is a reference point.

In the opposite direction, a genus g surface Σ along with two sets of embedded curves $\alpha = \{\alpha_1, \ldots, \alpha_g\}$ and $\beta = \{\beta_1, \ldots, \beta_g\}$ satisfying the first two properties in Definition 2.1.1 specifies uniquely a Heegaard decomposition $Y = U_0 \cup_\Sigma U_1$. (Thicken Σ and attach disks along the α_i and β_j curves; cap off the two remaining boundary components with three-balls.) If $z \in \Sigma - \alpha_1 - \cdots - \alpha_g - \beta_1 - \cdots - \beta_g$, then $(\Sigma, \alpha, \beta, z)$ is a pointed Heegaard diagram for Y.

Given a pointed Heegaard diagram $(\Sigma, \alpha, \beta, z)$, we introduce certain spaces that will be used in the definition of Heegaard Floer homology. Let $\mathrm{Sym}^g(\Sigma) = \Sigma \times \cdots \times \Sigma / S_g$ be the g-fold symmetric product of Σ. Here S_g is the permutation group on g elements. Inside $\mathrm{Sym}^g(\Sigma)$, the attaching circles α and β induce a pair of smoothly embedded, totally real g-dimensional tori $\mathbb{T}_\alpha = \alpha_1 \times \cdots \times \alpha_g$ and $\mathbb{T}_\beta = \beta_1 \times \cdots \times \beta_g$. The basepoint z induces a (complex codimension-one) submanifold

$$V_z = \{z\} \times \mathrm{Sym}^{g-1}(\Sigma) \subset \mathrm{Sym}^g(\Sigma).$$

Let $\mathbb{D}$ be the unit disk in $\mathbb{C}$. Let e_1, e_2 be the arcs in the boundary of $\mathbb{D}$ with $\mathrm{Re}(z) \geq 0$, $\mathrm{Re}(z) \leq 0$ respectively.

Definition 2.1.3. Given a pair of intersection points $x, y \in \mathbb{T}_\alpha \cap \mathbb{T}_\beta$, a *Whitney disk* connecting x to y is a continuous map

$$u : \mathbb{D} \to \mathrm{Sym}^g(\Sigma_g)$$

with the properties that $u(-i) = x$, $u(i) = y$, $u(e_1) \subset \mathbb{T}_\alpha$, $u(e_2) \subset \mathbb{T}_\beta$.

Let $\pi_2(x, y)$ denote the set of homotopy classes of Whitney disks connecting x to y. The set $\coprod_{x,y} \pi_2(x, y)$ is equipped with a multiplicative structure: If we take a Whitney disk connecting x to y, and one connecting

y to z, gluing them produces a disk connecting x to z. This operation gives rise to a multiplication

$$* : \pi_2(x, y) \times \pi_2(y, z) \to \pi_2(x, z).$$

Definition 2.1.4. Let x, $y \in \mathbb{T}_\alpha \cap \mathbb{T}_\beta$. For any point $z \in \Sigma - \alpha_1 - \cdots - \alpha_g - \beta_1 - \cdots - \beta_g$, let

$$n_z : \pi_2(x, y) \to \mathbb{Z}$$

denote the algebraic intersection number

$$n_z(\phi) = \#\phi^{-1}(\{z\} \times \mathrm{Sym}^{g-1}(\Sigma_g)).$$

Note that since $V_z = \{z\} \times \mathrm{Sym}^{g-1}(\Sigma_g)$ is disjoint from $\mathbb{T}_\alpha$ and $\mathbb{T}_\beta$, n_z is well-defined.

A closed oriented three-manifold Y has Euler characteristic zero, and so admits nowhere vanishing vector fields. The notion of Spin^c structures can be defined in every dimension, but in dimension three, it has an alternative description (due to Turaev [33]) in terms of nowhere vanishing vector fields.

Definition 2.1.5. Let v_1 and v_2 be two nowhere vanishing vector fields. We define an equivalence relation: v_1 is homologous to v_2 if there is a ball B in Y with the property that $v_1|_{Y-B}$ is homotopic to $v_2|_{Y-B}$. The space of Spin^c structures over Y, denoted Spin$^c(Y)$, is the set of nowhere vanishing vector fields modulo this relation.

The basepoint z determines a map

$$s_z \colon \mathbb{T}_\alpha \cap \mathbb{T}_\beta \to \mathrm{Spin}^c(Y)$$

which will be used in the construction of Heegaard Floer homology.

2.2 Heegaard Floer homology

Let $\mathcal{H} = (\Sigma, \alpha_1, \ldots, \alpha_g, \beta_1, \ldots, \beta_g, z)$ be a pointed Heegaard diagram for a rational homology three-sphere Y and let $\mathfrak{t} \in \mathrm{Spin}^c(Y)$. We recall the definitions of various versions of Heegaard Floer homology [25, 24]: $\widehat{\mathrm{HF}}(Y, \mathfrak{t})$, $\mathrm{HF}^+(Y, \mathfrak{t})$, $\mathrm{HF}^-(Y, \mathfrak{t})$, $\mathrm{HF}^\infty(Y, \mathfrak{t})$.

2.2.1 $\widehat{\mathrm{HF}}(Y,\mathfrak{t})$

We begin with the simplest version, the hat theory. The chain complex $\widehat{\mathrm{CF}}(\Sigma,\alpha,\beta,z,\mathfrak{t})$ is the free abelian group generated by intersection points $x \in \mathbb{T}_\alpha \cap \mathbb{T}_\beta$ with $s_z(x) = \mathfrak{t}$:

$$\widehat{\mathrm{CF}}(\Sigma,\alpha,\beta,z,\mathfrak{t}) = \bigoplus_{x\in\mathbb{T}_\alpha\cap\mathbb{T}_\beta, s_z(x)=\mathfrak{t}} \mathbb{Z}x.$$

The differential

$$\partial : \widehat{\mathrm{CF}}(\Sigma,\alpha,\beta,z,\mathfrak{t}) \to \widehat{\mathrm{CF}}(\Sigma,\alpha,\beta,z,\mathfrak{t})$$

is a signed count of points in $\mathfrak{M}(\phi)/\mathbb{R}$:

$$\partial x = \sum_{y\in\mathbb{T}_\alpha\cap\mathbb{T}_\beta} \sum_{\{\phi\in\pi_2(x,y)|\mu(\phi)=1, n_z(\phi)=0\}} \#\left(\frac{\mathfrak{M}(\phi)}{\mathbb{R}}\right) y.$$

Here, $\pi_2(x,y)$ denotes the space of homology classes of Whitney disks connecting x and y, $n_z(\phi)$ denotes the algebraic intersection number of a representative of ϕ with the codimension two submanifold $\{z\} \times \mathrm{Sym}^{g-1}(\Sigma) \subset \mathrm{Sym}^g(\Sigma)$, $\mathfrak{M}(\phi)$ denotes the moduli space of pseudo-holomorphic representatives of ϕ, and the *Maslov index* $\mu(\phi)$ denotes the expected dimension of $\mathfrak{M}(\phi)$.

To avoid dealing with signs, we often work over the base ring $\mathbb{Z}/2\mathbb{Z}$. In this case, $\widehat{\mathrm{CF}}(\Sigma,\alpha,\beta,z,\mathfrak{t}) = \oplus_{x\in\mathbb{T}_\alpha\cap\mathbb{T}_\beta}\mathbb{Z}/2\mathbb{Z}x$, and the differential counts the parity of the number of points in $\frac{\mathfrak{M}(\phi)}{\mathbb{R}}$.

The group $\widehat{\mathrm{CF}}(\Sigma,\alpha,\beta,z,\mathfrak{t})$ can be endowed with a relative (*Maslov*) grading

$$\mathrm{gr}(x,y) = \mu(\phi) - 2n_z(\phi),$$

where ϕ is any element $\phi \in \pi_2(x,y)$ and μ is the Maslov index.

It is proved in [25] that the differential ∂ squares to zero ($\partial^2 = 0$), and so puts a chain complex structure on $\widehat{\mathrm{CF}}(\Sigma,\alpha,\beta,z,\mathfrak{t})$.

The homology $H_*(\widehat{\mathrm{CF}}(\Sigma,\alpha,\beta,z,\mathfrak{t}))$ is independent of the choice of pointed Heegaard diagram for Y and the other choices in the definition (complex structures, perturbations):

Theorem 2.2.1 ([25])**.** *Let (Σ,α,β,z) and $(\Sigma',\alpha',\beta',z')$ be two pointed Heegaard diagrams for Y. Then the homology groups $H_*(\widehat{\mathrm{CF}}(\Sigma,\alpha,\beta,z,\mathfrak{t}))$ and $H_*(\widehat{\mathrm{CF}}(\Sigma',\alpha',\beta',z',\mathfrak{t}))$ are isomorphic.*

Theorem 2.2.1 allows us to define $\widehat{\mathrm{HF}}(Y,\mathfrak{t})$:

Definition 2.2.2. The Heegaard Floer homology group $\widehat{\mathrm{HF}}(Y,\mathfrak{t})$ is the homology of $\widehat{\mathrm{CF}}(\Sigma,\alpha,\beta,z,\mathfrak{t})$, where (Σ,α,β,z) is a Heegaard diagram for Y.

2.2.2 $\mathrm{HF}^\infty(Y,t)$

In this section, we introduce $\mathrm{CF}^\infty(\Sigma,\alpha,\beta,z,\mathfrak{t})$, which is generated as a free abelian group by $[x,i]$ where $x\in\mathbb{T}_\alpha\cap\mathbb{T}_\beta$ with $s_z(x)=\mathfrak{t}$ and $i\in\mathbb{Z}$. Again, the generators can be equipped with a relative grading

$$\mathrm{gr}([x,i],[y,j])=\mathrm{gr}(x,y)+2i-2j.$$

Let

$$\partial:\mathrm{CF}^\infty(\Sigma,\alpha,\beta,z,\mathfrak{t})\to\mathrm{CF}^\infty(\Sigma,\alpha,\beta,z,\mathfrak{t})$$

be the (differential) map defined by

$$\partial([x,i])=\sum_{y\in\mathbb{T}_\alpha\cap\mathbb{T}_\beta}\sum_{\{\phi\in\pi_2(x,y)|\mu(\phi)=1\}}\#\left(\frac{\mathfrak{M}(\phi)}{\mathbb{R}}\right)[y,i-n_z(\phi)].$$

There is an isomorphism $U:\mathrm{CF}^\infty(\Sigma,\alpha,\beta,z,\mathfrak{t})\to\mathrm{CF}^\infty(\Sigma,\alpha,\beta,z,\mathfrak{t})$ given by

$$U([x,i])=[x,i-1]$$

which lowers grading by two.

Equivalently, the chain complex $\mathrm{CF}^\infty(Y,\mathfrak{t})$ can be defined as the free $\mathbb{Z}[U,U^{-1}]$-module generated by the intersection points $\mathbb{T}_\alpha\cap\mathbb{T}_\beta$, with differential

$$\partial(x)=\sum_{y\in\mathbb{T}_\alpha\cap\mathbb{T}_\beta}\sum_{\{\phi\in\pi_2(x,y)|\mu(\phi)=1\}}\#\left(\frac{\mathfrak{M}(\phi)}{\mathbb{R}}\right)U^{n_z(\phi)}y.$$

The homology $\mathrm{HF}^\infty(\Sigma,\alpha,\beta,z,\mathfrak{t})$ only depends on (Y,t), and is denoted $\mathrm{HF}^\infty(Y,\mathfrak{t})$. It is proved in [24] that for rational homology three-spheres the homology $\mathrm{HF}^\infty(\Sigma,\alpha,\beta,z,\mathfrak{t})$ is always isomorphic to $\mathbb{Z}[U,U^{-1}]$. Although $\mathrm{HF}^\infty(Y,\mathfrak{t})$ is not an interesting invariant, a slight modification to the construction produces non-trivial invariants of rational homology three-spheres, as discussed in the following section.

2.2.3 $\mathrm{HF}^+(Y,\mathfrak{t})$ and $\mathrm{HF}^-(Y,\mathfrak{t})$

Let $\mathrm{CF}^-(\Sigma,\alpha,\beta,z,\mathfrak{t})$ denote the subcomplex of $\mathrm{CF}^\infty(\Sigma,\alpha,\beta,z,\mathfrak{t})$ freely generated by $[x,i]$ with $i<0$. Let $\mathrm{CF}^+(\Sigma,\alpha,\beta,z,\mathfrak{t})$ denote the quotient complex

$$\mathrm{CF}^+(\Sigma,\alpha,\beta,z,\mathfrak{t})=\mathrm{CF}^\infty(\Sigma,\alpha,\beta,z,\mathfrak{t})/\,\mathrm{CF}^-(\Sigma,\alpha,\beta,z,\mathfrak{t}).$$

There is a short exact sequence of chain complexes

$$0 \longrightarrow \mathrm{CF}^-(\Sigma,\alpha,\beta,z,\mathfrak{t}) \xrightarrow{i} \mathrm{CF}^\infty(\Sigma,\alpha,\beta,z,\mathfrak{t}) \xrightarrow{\pi} \mathrm{CF}^+(\Sigma,\alpha,\beta,z,\mathfrak{t}) \longrightarrow 0.$$

The map U restricts to an endomorphism on $\mathrm{CF}^-(\Sigma,\alpha,\beta,z,\mathfrak{t})$ which lowers grading by two. Hence U also restricts to an endomorphism on $\mathrm{CF}^+(\Sigma,\alpha,\beta,z,\mathfrak{t})$.

By identifying $\widehat{\mathrm{CF}}(\Sigma,\alpha,\beta,z,\mathfrak{t})$ with the subcomplex of $\mathrm{CF}^+(\Sigma,\alpha,\beta,z,\mathfrak{t})$ of generators $[x,i]$ with $i=0$, we get a short exact sequence

$$0 \longrightarrow \widehat{\mathrm{CF}}(\Sigma,\alpha,\beta,z,\mathfrak{t}) \longrightarrow \mathrm{CF}^+(\Sigma,\alpha,\beta,z,\mathfrak{t}) \xrightarrow{U} \mathrm{CF}^+(\Sigma,\alpha,\beta,z,\mathfrak{t}) \longrightarrow 0.$$

It is proved in [25] that the chain equivalences under (pointed) Heegaard moves on $\widehat{\mathrm{CF}}$ lift to chain equivalences on CF^∞, so the Floer homology groups $\mathrm{HF}^\pm(\Sigma,\alpha,\beta,z,t)$ are unchanged under pointed isotopies, handle slides, and stabilizations. This allows us to define the plus and minus versions of Heegaard Floer homology for a three-manifold Y equipped with a Spin^c structure $\mathfrak{t}$.

Definition 2.2.3. $\mathrm{HF}^\pm(Y,\mathfrak{t}) = \mathrm{HF}^\pm(\Sigma,\alpha,\beta,z,\mathfrak{t})$.

2.3 Knot Floer homology

A knot $K \subset Y$ can be specified by a *doubly-pointed Heegaard diagram* $(\Sigma,\alpha_1,\dots\alpha_g,\beta_1,\dots,\beta_g,z,w)$, where (Σ,α,β,z) is a pointed Heegaard diagram for Y, and w is an additional basepoint in $\Sigma\setminus\alpha\cup\beta$. The diagram represents the knot K via the following construction. Connect w and z via an arc γ_0 in $\Sigma-\alpha_1-\cdots-\alpha_g$. Connect w and z via another arc γ_1 in $\Sigma-\beta_1-\cdots-\beta_g$. By pushing γ_0 and γ_1 into the handlebodies U_0 and U_1 respectively, we obtain a knot $K\subset Y$.

2.3.1 $\widehat{\mathrm{HFK}}(K)$

Let K be a knot in S^3 and $(\Sigma_g,\alpha_1,\dots,\alpha_g,\beta_1,\dots,\beta_g,z,w)$ be a compatible doubly-pointed Heegaard diagram. Let $\widehat{\mathrm{CFK}}(K)$ be the free abelian group generated by intersection points $x\in\mathbb{T}_\alpha\cap\mathbb{T}_\beta$. Let the differential $\partial_K:\widehat{\mathrm{CFK}}(K)\to\widehat{\mathrm{CFK}}(K)$ be given by

$$\partial_K(x)=\sum_{y\in\mathbb{T}_\alpha\cap\mathbb{T}_\beta}\ \sum_{\{\phi\in\pi_2(x,y)\,|\,\mu(\phi)=1,n_z(\phi)=0,n_w(\phi)=0\}} \#\left(\frac{\mathfrak{M}(\phi)}{\mathbb{R}}\right)y.$$

Proposition 2.3.1 ([23, 31]). *$\partial_K^2 = 0$, making $\widehat{\mathrm{CFK}}(K)$ a chain complex. Its homology $\widehat{\mathrm{HFK}}(K)$ is independent of the choice of two-pointed Heegaard diagrams representing K, and the almost complex structures.*

The *Maslov grading* on $\widehat{\mathrm{CFK}}(K)$ is inherited from $\widehat{\mathrm{CF}}(Y)$: If x, $y \in \mathbb{T}_\alpha \cap \mathbb{T}_\beta$,

$$\mathrm{gr}(x, y) = \mu(\phi) - 2n_z(\phi)$$

where $\phi \in \pi_2(x, y)$ and μ is the Maslov index.

The additional basepoint w is used to define the relative *Alexander* grading on $\widehat{\mathrm{CFK}}(K)$:

$$A(x, y) = n_w(\phi) - n_z(\phi),$$

where $\phi \in \pi_2(x, y)$.

2.3.2 HFK^- and HFK^+

The chain complex $\mathrm{CFK}^-(K)$ is freely generated over $\mathbb{F}[U]$ by the set of intersection points in $\mathbb{T}_\alpha \cap \mathbb{T}_\beta$. The differential is defined as

$$\partial x = \sum_{y \in \mathbb{T}_\alpha \cap \mathbb{T}_\beta} \sum_{\phi \in \pi_2(x,y), \mu(\phi)=1} \#\, \mathfrak{M}(\phi)\, U^{n_w(\phi)} y.$$

This complex has a homological $\mathbb{Z}$-grading M, the *Maslov* grading, as well as a $\mathbb{Z}$-filtration A, the Alexander filtration. The relative Maslov and Alexander gradings are defined as follows. For generators x, $y \in \mathbb{T}_\alpha \cap \mathbb{T}_\beta$,

$$M(x) - M(y) = \mu(\phi) - 2n_w(\phi),$$

and

$$A(x) - A(y) = n_z(\phi) - n_w(\phi),$$

where $\phi \in \pi_2(x, y)$ is any domain. The relative Alexander grading of a linear combination $\sum_i x_i$ of generators is defined to be $\max_i\{A(x_i)\}$. The differential ∂ decreases Maslov grading by one and respects the Alexander filtration. That is,

$$M(\partial x) = M(x) - 1 \qquad \text{and} \qquad A(\partial x) \leq A(x).$$

Multiplication by U shifts the Maslov grading by two and respects the Alexander filtration:

$$M(Ux) = M(x) - 2 \qquad \text{and} \qquad A(Ux) = A(x) - 1.$$

Setting $U = 0$, we obtain the filtered chain complex $\widehat{\mathrm{CFK}}(K) = \mathrm{CFK}^-(K)/(U = 0)$. The total homology of $\widehat{\mathrm{CFK}}(K)$ is isomorphic to $\widehat{\mathrm{HF}}(S^3) = \mathbb{F}$. The normalization for the Maslov grading is chosen so that the generator for $\widehat{\mathrm{HF}}(S^3)$ lies in Maslov grading zero.

2.3.3 CFK^∞

The *full knot Floer chain complex*

$$\mathrm{CFK}^\infty(K) = \mathrm{CFK}^-(K) \otimes_{\mathbb{F}[U]} \mathbb{F}[U, U^{-1}]$$

is a $\mathbb{Z} \oplus \mathbb{Z}$-filtered chain complex, and its filtered chain homotopy equivalence type is a topological invariant of the knot K. $\mathrm{CFK}^\infty(K)$ is freely generated over $\mathbb{Z}$ by triples $[x, i, j]$, where $x \in \mathbb{T}_\alpha \cap \mathbb{T}_\beta$, $i, j \in \mathbb{Z}$, with $A(x) = j - i$. The triple $[x, i, j]$ corresponds to the generator $U^{-i}x$. Graphically, we can represent each generator of $\mathrm{CFK}^\infty(K)$ by a dot in the plane, with $[x, i, j]$ having coordinates (i, j). The j coordinate describes the Alexander grading of the generator, and the i coordinate describes the (negative of the) U power. The differentials are drawn by arrows. The action of U decreases Alexander grading by 1. The Maslov grading is not shown in the picture.

2.4 Concordance invariants and Heegaard Floer homology

Definition 2.4.1. The *smooth 4-ball genus* of a knot K is

$$g_4(K) = \min\{\mathrm{genus}(S) \mid S \subset \mathrm{B}^4 \text{ smoothly embedded surface}, \partial S = K\}.$$

A knot $K \subset S^3$ is *slice* if $g_4(K) = 0$. Two knots K_1 and K_2 are *(smoothly) concordant* if $K_1 \# -K_2$ is slice. Replacing the condition that the surface S is smoothly embedded with the condition of being *locally flat* gives the definition of *topologically slice knots* and *topological concordance*.

Let $\mathcal{C}$ denote the concordance group of knots, i.e. the set of knots in S^3 with the connect sum operation modulo concordance. Let $\mathcal{C}_{TS}$ be the subgroup of $\mathcal{C}$ generated by topologically slice knots. Endo [3] showed that $\mathcal{C}_{TS}$ contains an infinite rank subgroup, and Livingston [18] and Manolescu-Owens [19] showed that $\mathcal{C}_{TS}$ contains a $\mathbb{Z}^3$ summand using the smooth concordance homomorphisms τ of Ozsváth-Szabó [22], s of Rasmussen [32], and δ of Manolescu-Owens [19]. In [9] Hom uses knot Floer homology and the concordance invariant ϵ to show that $\mathcal{C}_{TS}$ contains a $\mathbb{Z}^\infty$ summand. The fact that the subgroup $\mathcal{C}_{TS}$ is highly non-trivial illustrates that there is a large difference between the smooth and topological categories. For example,

topologically slice but non-smoothly slice knots (i.e. nontrivial elements in $\mathcal{C}_{TS}$) give rise to exotic smooth structures on $\mathbb{R}^4$ (see, for example, [4]).

Heegaard Floer homology has proven to be a powerful tool in the study of knot concordance. In this section, we review the definitions of concordance invariants τ, ν, ν', and ν^+. Later, in Section 4.2 we review the definition of Hom's ϵ invariant. We focus on these particular ones because of their relevance to our work, specifically to Chapter 4 and Chapter 5 of this thesis.

Other concordance invariants coming from Heegaard Floer homology include Υ, $d(S^3_{\pm 1}(K))$, and d-invariants of double-branched covers, and are described in [21], [29], and [19, 12].

2.4.1 Cobordism maps on $\widehat{\mathrm{HF}}$

The complex $\mathrm{CFK}^\infty(K)$ is a $\mathbb{Z}\oplus\mathbb{Z}$-filtered complex. Given a subset $X \subset \mathbb{Z}\oplus\mathbb{Z}$, let CX denote the subgroup of $\mathrm{CFK}^\infty(K)$ generated by elements $[x,i,j]$ with filtration level $(i,j) \in X$.

Consider the chain map

$$\widehat{v}_s : C\{\max(i, j-s) = 0\} \to C\{i = 0\}$$

consisting of quotienting by $C\{i < 0, j = s\}$ followed by the inclusion. The large integer surgery formula of Ozsváth-Szabó [23] asserts that this map is induced by the two-handle addition cobordism $W_N(K)$ from $S^3_N(K)$ to S^3, where N is a sufficiently large positive integer. (It turns out $N > 2g(K) - 1$ suffices [23]). Let $\mathfrak{t}$ be the Spin^c structure on $W_N(K)$ such that

$$\langle c_1(\mathfrak{t}), [\widehat{F}]\rangle + N = 2s,$$

where $\widehat{F}$ is a capped-off Seifert surface for K.

Theorem 2.4.2 ([23]). *For $|s| \leq N/2$, the complex*

$$C\{\max(i, j-s) = 0\}$$

represents the complex $\widehat{\mathrm{CF}}(S^3_N(K), \mathfrak{s})$ and the map

$$\widehat{v}_{s*} : \widehat{\mathrm{HF}}(S^3_N(K), \mathfrak{s}) \to \widehat{\mathrm{HF}}(S^3)$$

is induced by the two-handle cobordism $W_N(K)$ with Spin^c structure $\mathfrak{t}$ where $\mathfrak{t}|_{S^3_N K} = \mathfrak{s}$.

Similarly, consider the chain map

$$\widehat{v}'_s : C\{i = 0\} \to C\{\min(i, j - s) = 0\}$$

consisting of quotienting by $C\{i = 0, j \leq s\}$ followed by the inclusion. The negative large integer surgery formula of Ozsváth-Szabó [23] asserts that this map is induced by the two-handle addition cobordism $W_{-N}(K)$ from $S^3_{-N}(K)$ to S^3, where N is a sufficiently large positive integer. (It turns out $N > 2g(K) - 1$ suffices [23]). Let $\mathfrak{t}$ be the Spin^c structure on $W_{-N}(K)$ such that

$$\langle c_1(\mathfrak{t}), [\widehat{F}]\rangle - N = 2s,$$

where $\widehat{F}$ is a capped-off Seifert surface for K.

Theorem 2.4.3 ([23]). *For $|s| \leq N/2$, the complex*

$$C\{\min(i, j - s) = 0\}$$

represents the complex $\widehat{\mathrm{CF}}(S^3_{-N}(K), s)$ and the map

$$\widehat{v}'_{s*} : \widehat{\mathrm{HF}}(S^3_{-N}(K), s) \to \widehat{\mathrm{HF}}(S^3)$$

is induced by the two-handle cobordism $W_{-N}(K)$ with Spin^c structure $\mathfrak{t}$ where $\mathfrak{t}|_{S^3_{-N}K} = \mathfrak{s}$.

2.4.2 The Ozsváth-Szabó τ invariant

A knot induces a $\mathbb{Z}$-filtration (the Alexander filtration) on the Floer chain complex $\widehat{\mathrm{CF}}(S^3)$. The Ozsváth-Szabó invariant τ [22] measures the minimum $\mathbb{Z}$-filtration level on which the total homology $\widehat{\mathrm{HF}}(S^3) \cong \mathbb{Z}$ is supported.

Definition 2.4.4 ([22]).

$$\tau(K) = \min\{s \in \mathbb{Z} \mid i_s : H_*(C\{i = 0, j \leq s\}) \to H_*(C\{i = 0\}) \text{ is an isomorphism}\}.$$

Note that $H_*(C\{i = 0\}) \cong \widehat{\mathrm{HF}}(S^3) \cong \mathbb{Z}$, so the condition that the map i_s is an isomorphism is equivalent to i_s being nontrivial.

Theorem 2.4.5 ([22]). *The map $\tau : \mathcal{C} \to \mathbb{Z}$ is a surjective homomorphism.*

Theorem 2.4.6 ([22])**.** *The absolute value of τ is a lower bound on the smooth four-ball genus of a knot. That is, $|\tau(K)| \leq g_4(K)$.*

The Milnor conjecture, originally proved by Kronheimer and Mrowka [13] using gauge theory, states that the unknotting number and four-ball genus of a torus knot $T_{p,q}$ is $(p-1)(q-1)/2$. Ozsváth and Szabó used the invariant τ to give an alternative proof [22] of the Milnor conjecture.

2.4.3 The concordance invariants ν and ν'

Definition 2.4.7 ([28], Section 9)**.** The concordance invariant $\nu(K)$ is defined as

$$\nu(K) = \min\{s \in \mathbb{Z} \mid \widehat{v}_{s*} \text{ is nontrivial}\}.$$

Definition 2.4.8. The concordance invariant $\nu'(K)$ is defined as

$$\nu'(K) = \max\{s \in \mathbb{Z} \mid \widehat{v}'_{s*} \text{ is nontrivial}\}.$$

The map $\widehat{v}_{s*}$ is trivial for $s < \tau(K)$ and nontrivial for $s > \tau(K)$. It follows that $\nu(K)$ is either $\tau(K)$ or $\tau(K)+1$. The map $\widehat{v}'_{s*}$ is trivial for $s > \tau(K)$ and nontrivial for $s < \tau(K)$. It follows that $\nu'(K)$ is either $\tau(K)$ or $\tau(K)-1$. Together, ν and ν' give the same information as ϵ and τ, where ϵ is reviewed in Section 4.2.

2.4.4 Cobordism maps on HF^+

Consider the chain map

$$v_s^+ : C\{\max(i, j-s) \geq 0\} \to C\{i \geq 0\}$$

consisting of quotienting by $C\{i < 0, j \geq s\}$ followed by the inclusion. The large integer surgery formula of Ozsváth-Szabó [23] asserts that this map is induced by the two-handle addition cobordism $W_N(K)$ from $S^3_N(K)$ to S^3, where N is a sufficiently large positive integer. ($N > 2g(K) - 1$ suffices [23]). Let $\mathfrak{t}$ be the Spin^c structure on $W_N(K)$ such that

$$\langle c_1(\mathfrak{t}), [\widehat{F}]\rangle + N = 2s,$$

where $\widehat{F}$ is a capped-off Seifert surface for K.

Theorem 2.4.9 ([23])**.** *For $|s| \leq N/2$, the complex*

$$C\{\max(i, j-s) \geq 0\}$$

represents the complex $\mathrm{CF}^+(S^3_N(K), s)$ *and the map*

$$v^+_{s*} : \mathrm{HF}^+(S^3_N(K), s) \to \mathrm{HF}^+(S^3)$$

is induced by the two handle cobordism $W_N(K)$ *with Spin*^{c} *structure* $\mathfrak{t}$ *where* $\mathfrak{t}|_{S^3_N K} = \mathfrak{s}$.

2.4.5 The Hom-Wu ν^+ invariant

For a rational homology 3-sphere Y with a Spin^c structure $\mathfrak{s}$, $\mathrm{HF}^+(Y, \mathfrak{s})$ can be decomposed as the direct sum of two groups: the first group is the image of $\mathrm{HF}^\infty(Y, \mathfrak{s}) \cong \mathbb{F}[U, U^{-1}]$ in $\mathrm{HF}^+(Y, \mathfrak{s})$, which is isomorphic to $\mathfrak{T}^+ = \mathbb{F}[U, U^{-1}]/U\mathbb{F}[U]$; the second group is $\mathrm{HF}_{\mathrm{red}}(Y, \mathfrak{s}) = \mathrm{HF}^+(Y, \mathfrak{s})/\mathfrak{T}^+$. That is,

$$\mathrm{HF}^+(Y, \mathfrak{s}) = \mathfrak{T}^+ \oplus \mathrm{HF}_{\mathrm{red}}(Y, \mathfrak{s}).$$

Definition 2.4.10 ([11])**.** The concordance invariant ν^+ is defined as

$$\nu^+(K) = \min\{s \mid v^+_{s*} : \mathrm{HF}^+(S^3_N(K), \mathfrak{s}) \to \mathrm{HF}^+(S^3) \text{ sends 1 to 1}\}$$

where 1 denotes the lowest graded generator in the subgroup $\mathfrak{T}^+$ of the homology, and N is sufficiently large so that the integer surgery formula holds.

Some properties of ν^+ shown in [11] are

$$\tau(K) \leq \nu(K) \leq \nu^+(K)$$

and $\nu^+(K) \geq 0$. In addition, ν^+ gives a lower bound on the four-ball genus:

Theorem 2.4.11 ([11])**.** $\nu^+(K) \leq g_4(K)$.

Furthermore, in [11] Hom and Wu provide a family of knots where $\nu^+(K)$ is an arbitrarily better bound on $g_4(K)$ than $\tau(K)$ (or $\nu(K)$ or $\nu'(K)$).

2.4.6 The concordance invariant $\nu^{+'}$

We introduce a concordance invariant $\nu^{+'}$, so that the pair ν^+ and $\nu^{+'}$ is the HF^+ analogue to the pair ν and ν' in the hat theory.

Definition 2.4.12. Let $-N$ be sufficiently negative so that the negative large integer surgery formula holds.

$$\nu^{+'}(K) = \max\{s \in \mathbb{Z} \mid v_{s*}^{+'} : \mathrm{HF}^+(S^3) \to \mathrm{HF}^+(S^3_{-N}(K), \mathfrak{s}) \text{ is injective}\}$$

An equivalent definition of $\nu^{+'}(K)$ uses the invariant ν^+ of the mirror of K:

Lemma 2.4.13. $\nu^{+'}(K) = \nu^+(-K)$.

Proof. Recall the symmetry of CFK^∞ under mirroring ([23], Section 3.5):

$$\mathrm{CFK}^\infty(-K) \simeq \mathrm{CFK}^\infty(K)^*$$

where $\mathrm{CFK}^\infty(K)^*$ is the dual complex $\mathrm{Hom}_{\mathbb{F}[U,U^{-1}]}(\mathrm{CFK}^\infty(K), \mathbb{F}[U,U^{-1}])$. The following conditions are equivalent:

$$\begin{aligned}
& v_{s*}^{+'} \colon \mathrm{HF}^+(S^3) \to \mathrm{HF}^+(S^3_{-N}(K), \mathfrak{s}) \text{ is injective,} \\
\iff \quad & v_{s*}^{-'} \colon \mathrm{HF}^-(S^3) \to \mathrm{HF}^-(S^3_{-N}(K), \mathfrak{s}) \text{ is injective,} \\
\iff \quad & v_{s*}^{+} \colon \mathrm{HF}^+(S^3_{-N}(-K), \mathfrak{s}) \to \mathrm{HF}^+(S^3) \text{ sends 1 to 1,}
\end{aligned}$$

where 1 denotes the lowest graded generator of the subgroup $\mathfrak{T}^+$ in homology. □

It follows from the above lemma that the invariant $\nu^{+'}$ exhibits properties similar to ν^+:

$$\nu^{+'}(K) \leq \nu'(K) \leq \tau(K)$$

and $\nu^{+'}(K) \leq 0$. In addition, the absolute value of $\nu^{+'}$ gives a lower bound on the four-ball genus.

Theorem 2.4.14. $|\nu^{+'}(K)| \leq g_4(K)$

Proof. This follows from the fact that $\nu^+(K) \leq g_4(K)$ and Lemma 2.4.13. □

Chapter 3

Bordered Floer Homology and Generalized Whitehead Doubles

3.1 Background on Bordered Floer Homology for three-manifolds with torus boundary

Bordered Floer theory, introduced by Lipshitz, Ozsváth, and Thurston in [16], is a version of Heegaard Floer theory for three-manifolds with one- or two-component boundary and is a major tool for computing Heegaard Floer invariants for closed three-manifolds. After cutting a three-manifold into simpler pieces, bordered Floer theory gives a way to algorithmically compute the hat version of Heegaard Floer homology $\widehat{\mathrm{HF}}(Y)$ with $\mathbb{Z}/2\mathbb{Z}$ of any closed three-manifold Y.

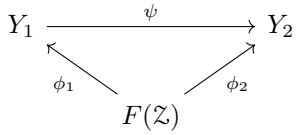
In this section, we review bordered Floer homology for the special case of three-manifolds with one torus boundary component.

Definition 3.1.1. A *pointed matched circle* $\mathcal{Z} = \{Z, z, \{a_1, a_1'\}, \{a_2, a_2'\}\}$ that specifies a once-punctured genus one surface (a punctured torus) consists of a circle Z, marked points a_1, a_2, a_1', a_2', $z \in Z$, in that order as we traverse Z clockwise.

A pointed matched circle $\mathcal{Z} = \{Z, z, \{a_1, a_1'\}, \{a_2, a_2'\}\}$ specifies a punctured torus $T^2 \setminus D^2$ as follows. Thicken Z to $Z \times [0,1]$. Attach a two-dimensional one-handle α_1^a (resp. α_2^a) to $a_1 \times \{0\}$ and $a_1' \times \{0\}$ (resp. $a_2 \times \{0\}$ and $a_2' \times \{0\}$). The result has boundary $(Z \times \{1\}) \sqcup (Z \times \{0\})$. Fill in $Z \times \{0\}$ with a disk D^2. The result is $F^\circ(\mathcal{Z}) = T^2 \setminus D^2$. Filling in $Z \times \{1\}$ with a disk D^2 results in a closed boundary torus $F(\mathcal{Z}) = T^2$.

Definition 3.1.2. A *bordered three-manifold* consists of a compact, oriented three-manifold Y with boundary ∂Y and a homeomorphism $\phi : F(\mathcal{Z}) \to \partial Y$ for some pointed matched circle $\mathcal{Z}$.

Call two bordered three-manifolds $(Y_1, \phi_1 : F(\mathcal{Z}) \to \partial Y_1)$ and $(Y_2, \phi_2 : F(\mathcal{Z}) \to \partial Y_2)$ equivalent if there is a homeomorphism $\psi : Y_1 \to Y_2$ so that $\phi_2 = \psi \circ \phi_1$, i.e. the diagram



commutes.

Analogous to Heegaard diagrams that are used to combinatorially represent closed three-manifolds, *bordered* Heegaard diagrams combinatorially represent three-manifolds with parametrized boundary, or *bordered three-manifolds*.

Definition 3.1.3. Let $\mathcal{Z}$ be a pointed matched circle representing a (punctured) torus. A *bordered Heegaard diagram* with boundary $\mathcal{Z}$ is a tuple

$$(\Sigma_g, \alpha_1^a, \alpha_2^a, \alpha_1^c \ldots, \alpha_{g-1}^c, \beta_1, \ldots, \beta_g, z)$$

where

- Σ_g is a compact oriented surface of genus g with one boundary component.
- $\beta = \{\beta_1, \ldots, \beta_g\}$ is a g-tuple of pairwise disjoint circles in the interior of Σ.
- $\alpha^c = \{\alpha_1^c, \ldots, \alpha_{g-1}^c\}$ is a $(g-1)$-tuple of pairwise disjoint circles in the interior of Σ.
- $\alpha^a = \{\alpha_1^a, \alpha_2^a\}$ is a pair of disjoint arcs in Σ with boundary in $\partial\Sigma$.
- z is a basepoint in $\partial\Sigma \setminus \alpha^a$.
- $\alpha^a \cap \alpha^c = \emptyset$.
- $\Sigma \setminus (\alpha^a \cup \alpha^c)$ and $\Sigma \setminus \beta$ are both connected.
- $\mathcal{Z} = (\partial\Sigma, z, \{\alpha_1^a \cap \partial\Sigma\}, \{\alpha_2^a \cap \partial\Sigma\})$

Let $\mathcal{H} = (\Sigma_g, \alpha_1^a, \alpha_2^a, \alpha_1^c \ldots, \alpha_{g-1}^c, \beta_1, \ldots, \beta_g, z)$ be a bordered Heegaard diagram with boundary $\mathcal{Z}$. Construct the corresponding bordered three-manifold $Y(\mathcal{H})$ as follows.

(1) Thicken Σ to $\Sigma \times [0, 1]$.

(2) Attach three-dimensional two-handles along the α^c-circles in $\Sigma \times \{0\}$.

(3) Attach three-dimensional two-handles along the β-circles in $\Sigma \times \{1\}$.

A parameterization of the boundary is specified as follows. Consider the graph

$$(\alpha_1^a \cup \alpha_2^a \cup (\partial\Sigma \setminus \mathrm{nbd}(z))) \times \{0\} \subset \Sigma \times \{0\},$$

thought of as a subset of ∂Y. The closure F° of a neighborhood of this graph is naturally identified with $F^\circ(\mathcal{Z})$. The complement of F° in ∂Y is a disk, and is identified with $F(\mathcal{Z}) \setminus F^\circ(\mathcal{Z})$.

A *doubly-pointed bordered Heegaard diagram*, or a bordered Heegaard diagram with two basepoints z and w, represents a knot inside a bordered three-manifold, with the restriction that a point on the knot lies on the boundary. The construction of the knot is the same as in the case of doubly-pointed Heegaard diagrams for closed three-manifolds.

In the case of three-manifolds with torus boundary, bordered Floer homology assigns to a pointed matched circle $\mathcal{Z}$ a graded algebra $\mathcal{A}(\mathcal{Z})$.

Definition 3.1.4. The algebra $A(T^2) = A(\mathcal{Z})$ associated to the unique pointed matched circle $\mathcal{Z}$ for T^2 is given by the path algebra with relations

$$\iota_1 \overset{\rho_1,\rho_3}{\underset{\rho_2}{\rightleftarrows}} \iota_2 \quad / \ (\rho_2\rho_1 = \rho_3\rho_2 = 0).$$

To a bordered three-manifold $(Y, \phi\colon F(\mathcal{Z}) \to \partial Y)$, bordered Floer theory associates a right A_∞-module $\widehat{\mathrm{CFA}}(Y)$ over the algebra $\mathcal{A}(\mathcal{Z})$ and a Type D structure $\widehat{\mathrm{CFD}}(Y)$. See [16] for definitions of these invariants.

Let Y_1 and Y_2 be two bordered three-manifolds whose boundaries $\partial Y_1 \cong -\partial Y_2 \cong F(\mathcal{Z})$ are glued together, to produce the closed three-manifold Y. The pairing theorem of bordered Floer homology theory states that there exists a chain homotopy equivalence between $\widehat{\mathrm{CF}}(Y)$ and the boxed tensor product of $\widehat{\mathrm{CFA}}(Y_1) \boxtimes \widehat{\mathrm{CFD}}(Y_2)$:

Theorem 3.1.5 ([16])**.** *Let $Y = Y_1 \cup Y_2$, where Y_1 and Y_2 are bordered three-manifolds whose boundaries are glued together to produce the closed three-manifold Y. Then*

$$\widehat{\mathrm{CF}}(Y) \simeq \widehat{\mathrm{CFA}}(Y_1) \boxtimes \widehat{\mathrm{CFD}}(Y_2).$$

Bordered Floer homology is useful for studying satellite knots. Suppose $\mathcal{H}_1$ is a bordered Heegaard diagram for a knot complement $S^3 \setminus \mathrm{nbd}(K)$ with 0-framing of the boundary. Let $\mathcal{H}_2$ denote a doubly-

pointed bordered Heegaard diagram for a knot inside a solid torus $\mathbb{D}^2 \times S^2$ with 1-framing. Then $\mathcal{H}_1 \cup_\partial \mathcal{H}_2$ is a doubly-pointed Heegaard diagram representing a knot L in S^3.

Given a doubly-pointed bordered Heegaard diagram $\mathcal{H}$, let $\mathrm{CFD}^-(\mathcal{H}) = \mathbb{F}_2[U] \otimes_{\mathbb{F}_2} \widehat{\mathrm{CFD}}(\mathcal{H})$ with differential given by

$$\partial x = \sum_{y \in \mathfrak{S}(\mathcal{H})} \sum_{n \geq 0} \sum_{(\rho_1, \ldots, \rho_n)} \sum_{B | \mathrm{ind}(B, \rho_1, \ldots, \rho_n) = 1} \left(\#\mathcal{M}^B(x, y; \rho_1, \ldots, \rho_n)\right) a(-\rho_1) \cdots a(-\rho_n) U^{n_w(B)} y$$

Theorem 3.1.6 ([17]). *With notation as above, the knot Floer homology of the satellite knot $L \subset S^3$ is determined by the pairing*

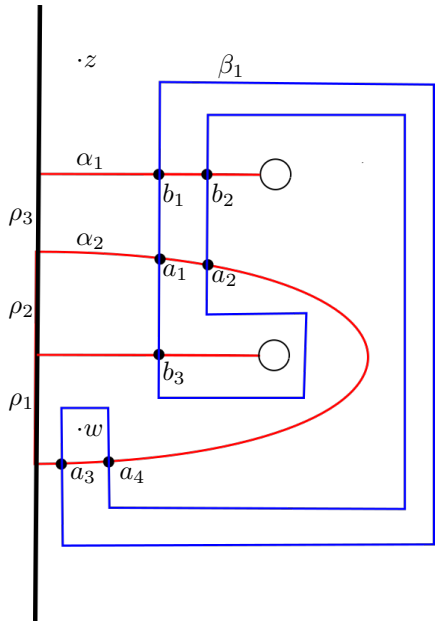
$$g\,\mathrm{CFK}^-(L) \cong \mathit{Mor}(\widehat{\mathrm{CFD}}(-\mathcal{H}_1), \mathrm{CFD}^-(\mathcal{H}_2, z, w)).$$

3.2 Bordered Floer Homology and Whitehead Doubles

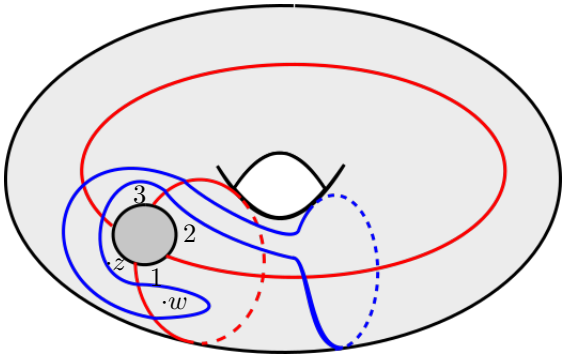
The positively-clasped (resp. negatively-clasped) t-twisted Whitehead double of a knot is denoted by $D_+(K,t)$ (resp. $D_-(K,t)$). The pattern knot for a positively-clasped (resp. negatively-clasped) 0-twisted Whitehead double $W(0;1)$ (resp. $W(0;-1)$) is shown in Figure 3.6 with $n = 1$ (resp. $n = -1$). The knot Floer homology of Whitehead doubles was studied by Hedden [5].

A doubly-pointed genus one bordered Heegaard diagram $\mathcal{H} = (\Sigma, \beta, \alpha_1, \alpha_2, w, z)$ is shown in Figure 3.1. The diagram $\mathcal{H}$ induces $(\mathbb{D}^2 \times S^1, W(0;-1))$. That is, the three-manifold $Y(\mathcal{H})$ represented by $\mathcal{H}$ is a solid torus $\mathbb{D}^2 \times S^1$, and the knot is the negatively-clasped Whitehead double pattern knot $W(0;-1)$. We verify that this diagram represents a negatively-clasped Whitehead double pattern knot in $Y(\mathcal{H})$ by following the method in Construction 4.8 in [17]. We draw an arc η to connect w and z in the complement of the β circle, and another arc γ to connect w and z in the complement of the α_1 and α_2 curves. Viewing Σ as $\Sigma \times \{1/2\}$ inside $\Sigma \times [0,1] \subset Y(\mathcal{H})$, let γ' be the result of pushing the interior of γ slightly into $\Sigma \times [0, 1/2)$ and let η' be the result of pushing the interior of η into $\Sigma \times (1/2, 1]$. We end up with a pattern knot $\gamma' \cup \eta'$ as illustrated in Figure 3.1, the negatively-clasped Whitehead double pattern $W(0;-1)$.

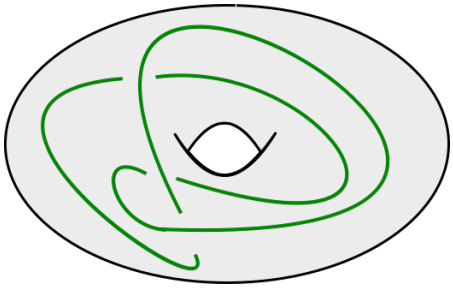
The type D module CFD^- associated to the bordered Heegaard diagram in Figure 3.1 has seven generators: $\{b_1, b_2, b_3\}$ and $\{a_1, a_2, a_3, a_4\}$ corresponding to intersection points $\beta \cap \alpha_1$ and $\beta \cap \alpha_2$. Since the (bordered) Heegaard surface has genus one, the differential maps of CFD^- count immersed disks of index one. Moreover, by lifting to the universal abelian cover $\mathbb{R}^2 \setminus \mathbb{Z}^2$ of the punctured torus, we can instead count *embedded* disks of index one. The index one condition implies that each corner must be less than 180°. It is clear from the diagram of the universal cover (Figure 3.4) that all the disks in the differential of



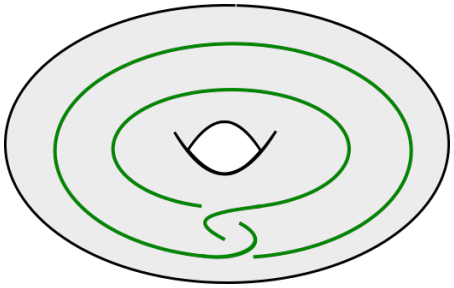
(a) Bordered Heegaard diagram for negatively-clasped Whitehead double pattern knot $W(0;-1)$ in a punctured solid torus



(b) Bordered Heegaard diagram for negatively-clasped Whitehead double pattern knot $W(0;-1)$ in a punctured solid torus



(c) Negatively-clasped Whitehead double pattern knot $W(0;-1)$ in a solid torus



(d) Negatively-clasped Whitehead double pattern knot $W(0;-1)$ in a solid torus

Figure 3.1: Doubly-pointed Bordered Heegaard diagram and pattern knot for negatively-clasped Whitehead double

$\mathrm{CFD}^-(W(0;-1))$ are depicted in Figure 3.5. The differential ∂ for $\mathrm{CFD}^-(W(0;-1))$ is given in Figure 3.2. After a change of basis, $\mathrm{CFD}^-(W(0;-1))$ splits into two summands, see Figure 3.3.

In [5], Hedden computes the knot Floer homology $\widehat{\mathrm{HFK}}(D_+(K,t)$, the filtered chain homotopy type $\mathcal{F}(D_+(K,t))$ and $\tau(D_+(K,t))$ in terms of the original filtered knot Floer chain complex $\mathcal{F}(K,i)$ and $\tau(K)$.

Theorem 3.2.1 ([5] Theorem 1.4)**.** $\tau(D_+(K,t)) = \begin{cases} 0 & \text{for } t \geq 2\tau(K); \\ 1 & \text{for } t < 2\tau(K). \end{cases}$

$$
\begin{aligned}
\partial b_1 &= Ub_2 + \rho_3 a_1 + U\rho_{123} a_3 + U\rho_{123} a_2 \\
\partial b_2 &= \rho_3 a_2 + U\rho_{123} a_4 \\
\partial b_3 &= U\rho_1 a_2 \\
\partial a_1 &= \rho_2 b_3 + U a_2 \\
\partial a_2 &= 0 \\
\partial a_3 &= U a_4 \\
\partial a_4 &= 0
\end{aligned}
$$

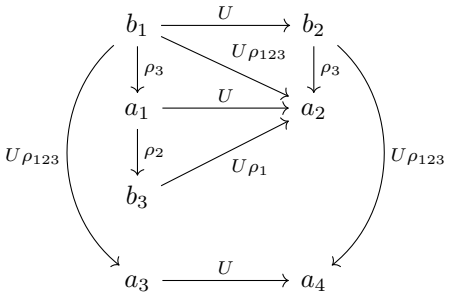


Figure 3.2: $\mathrm{CFD}^-(W(0;-1))$

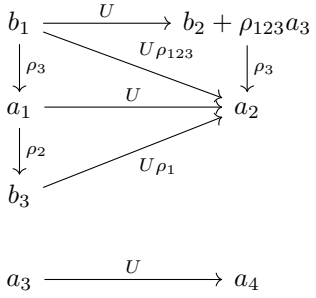


Figure 3.3: $\mathrm{CFD}^-(W(0;-1))$ after a change of basis

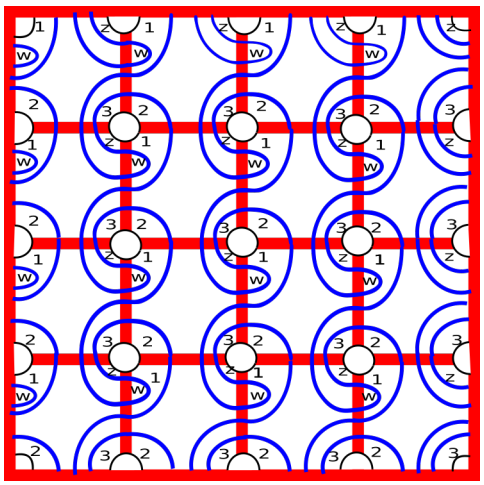


Figure 3.4: A lift of the doubly-pointed bordered Heegaard diagram for a punctured torus with the negatively-clasped Whitehead double pattern knot to the universal abelian cover $\mathbb{R}^2 \setminus \mathbb{Z}^2$

The red curves are lifts of α_1 and α_2 and the blue are lifts of the β_1 circle in Figure 3.1(a).

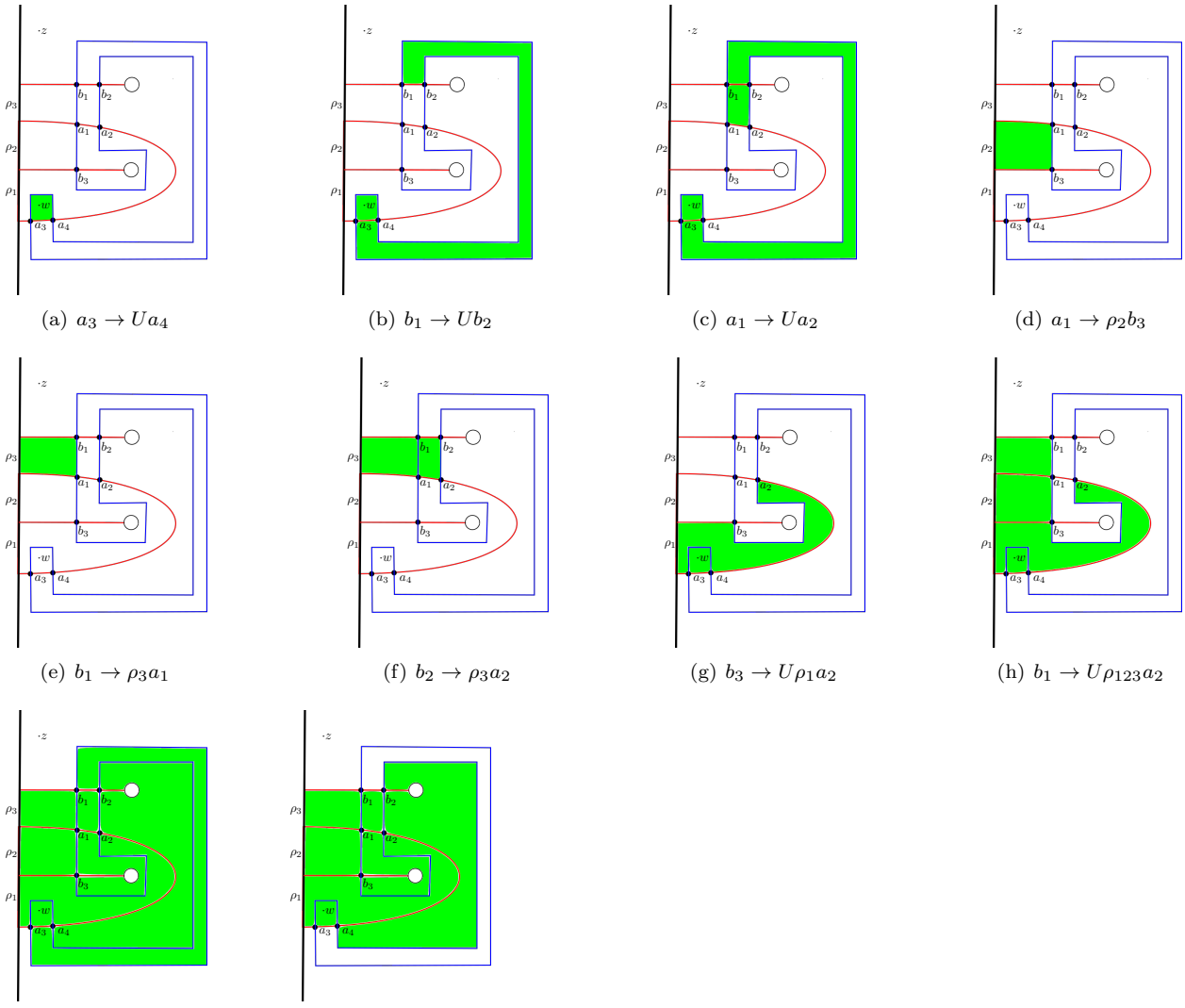


Figure 3.5: Counting immersed disks in $\mathrm{CFD}^-(W(0;-1))$ in a bordered Heegaard diagram for a punctured torus with a Whitehead double pattern
The disks in (i) and (j) contain the three separate chords ρ_1, ρ_2, and ρ_3. The eight other disks contain a single Reeb chord.

3.3 Generalized Whitehead Doubles

We introduce a family of satellite knots $W(K,t;n)$ indexed by two parameters, t, the twisting coefficient, and n, the number of full twists in the clasp region. Figure 3.6 shows the pattern knot inside a solid torus, and Figure 3.7 shows the generalized Whitehead double of a right-handed trefoil. The satellite knot $W(K,t;1)$ (resp. $W(K,t;-1)$) is the ordinary Whitehead double $D_+(K,t)$ (resp. $D_-(K,t)$) of K. We call these knots t-twisted, n-clasped generalized Whitehead doubles.

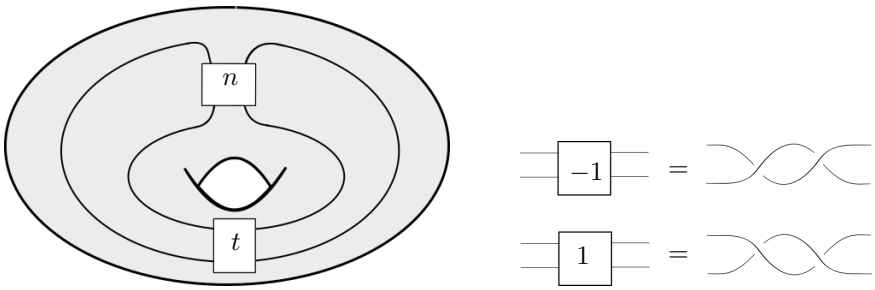


Figure 3.6: Pattern knot $W(t;n)$ for the t-twisted n-clasped generalized Whitehead double $W(K,t;n)$

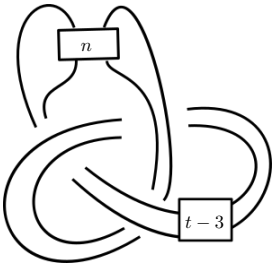


Figure 3.7: The $(t-3)$-twisted n-clasped generalized Whitehead double of the right-handed trefoil
The shift by three full twists in the projection of $W(\mathrm{RHT},t;n)$ arise from the writhe, $w(\mathrm{RHT})=3$, of the trefoil.

By using bordered Floer homology, we compute τ of these satellite knots in terms of τ of a companion knot. Our results agree with those of Levine [15].

Figure 3.8 shows a doubly-pointed genus one bordered Heegaard diagrams for the -2-clasped generalized Whitehead double $W(0;-2)$ pattern knot. Figure 3.9 depicts a sequence of pattern knots that demonstrates the method in Construction 4.8 in [17] indeed produces the pattern knot $W(0;-2)$.

The generators for the type D module $\mathrm{CFD}^-(W(0;-2))$ are intersection points $\beta_1\cap\alpha_1$ and $\beta_1\cap\alpha_2$. They consist of the original seven generators $\{a_1,a_2,a_3,a_4,b_1,b_2,b_3\}$ from the diagram in Figure 3.1, as well as eight new generators: $\{h_1,h_2,g_1,g_2,f_1,f_2,e_1,e_2\}$. By lifting the bordered diagram to the universal cover $\mathbb{R}^2\setminus\mathbb{Z}^2$ as in Figure 3.10, and counting embedded disks of index one, one sees all the disks in the differential of $\mathrm{CFD}^-(W(0;-2))$. Figure 3.13 depicts the immersed disks of index one with $n_z(\phi)=0$ counted in the differential of $\mathrm{CFD}^-(W(0;-2))$. The differential ∂ is given by Figure 3.11. After performing a simple change of basis, one sees in Figure 3.12 that $\mathrm{CFD}^-(W(0;-2))$ contains a $\mathrm{CFD}^-(W(0;-1))$ summand.

Proposition 3.3.1. $\mathrm{CFD}^-(W(0;-(n+1)))$ *contains a* $\mathrm{CFD}^-(W(0;-1))$ *summand.*

Proof. Figure 3.14 depicts a bordered Heegaard diagram for the $-(n+1)$-clasped generalized Whitehead double $W(0;-(n+1))$. $\mathrm{CFD}^-(W(0;-(n+1)))$ contains $8n$ generators $\{h_1,\dots,h_{2n},\ g_1,\dots g_{2n},\ f_1,\dots f_{2n},\ e_1,\dots e_{2n}\}$, in addition to seven generators $\{a_1,a_2,a_3,a_4,b_1,b_2,b_3\}$ that can be identified with those in $\mathrm{CFD}^-(W(0;-1))$. By lifting the bordered diagram to the universal cover $\mathbb{R}^2\setminus\mathbb{Z}^2$, the differential

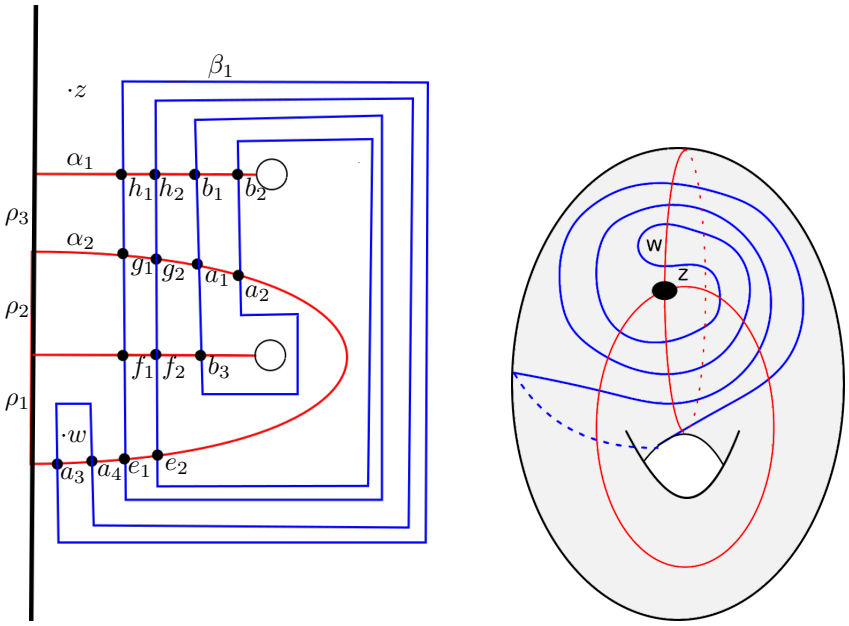
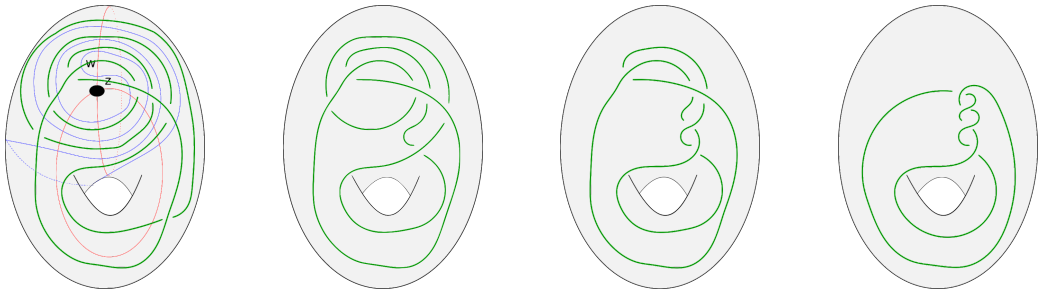


Figure 3.8: Doubly-pointed bordered Heegaard diagram for a -2-clasped Whitehead double pattern knot $W(0;-2)$ in a punctured solid torus



(a) (b) (c) (d)

Figure 3.9: Pattern knot
This sequence of pictures shows that the pattern knot in Figure 3.8 is $W(0;-2)$, the negatively twice-clasped Whitehead double.

in $\mathrm{CFD}^-(W(0;-(n+1)))$ counts embedded disks of index one with $n_z(\phi) = 0$. Figure 3.15 shows $\mathrm{CFD}^-(W(0;-(n+1)))$.

After a simple change of basis that replaces b_2 with $b_2 + \rho_{123}e_{2n-1}$ and h_2 with $h_2 + \rho_{123}a_3$, a summand that is isomorphic to $\mathrm{CFD}^-(W(0;-1))$ splits off the rest of the type D module. In conclusion, CFD^- of a generalized Whitehead double pattern knot contains a summand that is $\mathrm{CFD}^-(W(0;-1))$. □

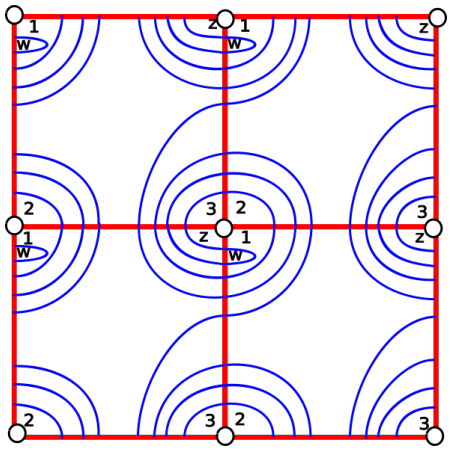


Figure 3.10: A lift of the doubly-pointed bordered Heegaard diagram for a punctured torus with the negatively twice-clasped Whitehead double pattern knot to the universal cover $\mathbb{R}^2 \setminus \mathbb{Z}^2$

$$
\begin{aligned}
\partial b_1 &= Ub_2 + \rho_3 a_1 + U\rho_{123}(e_1 + a_2) \\
\partial b_2 &= \rho_3 a_2 + U\rho_{123} e_2 \\
\partial b_3 &= U\rho_1 a_2 \\
\partial a_1 &= \rho_2 b_3 + U a_2 \\
\partial a_3 &= U a_4 \\
\partial h_1 &= Uh_2 + \rho_3 g_1 + U\rho_{123}(e_1 + a_3) \\
\partial h_2 &= \rho_3 g_2 + U\rho_{123}(e_2 + a_4) \\
\partial f_1 &= U f_2 + U\rho_1 e_1 \\
\partial f_2 &= U\rho_1 e_2 \\
\partial g_1 &= U g_2 + \rho_2 f_1 \\
\partial g_2 &= \rho_2 f_2 \\
\partial e_1 &= U e_2 \\
\partial a_2 &= \partial a_4 = \partial e_2 = 0
\end{aligned}
$$

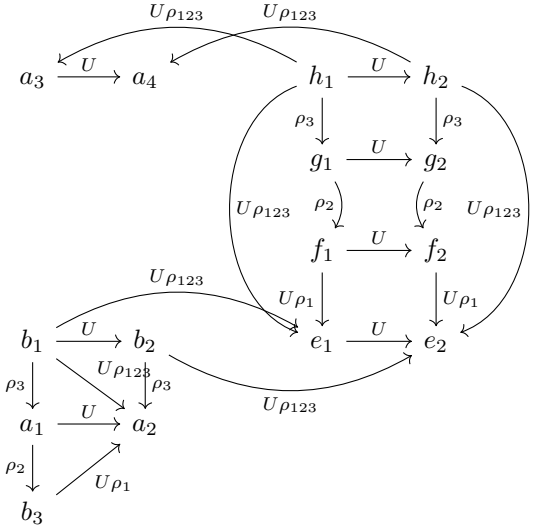


Figure 3.11: The type D module $\mathrm{CFD}^-(W(0;-2))$

Theorem 3.3.2. *Let $W(K,t;n)$ denote the t-twisted, n-clasped generalized Whitehead double of K.*

$$
\tau(W(K,t;n)) = \begin{cases} -1, & \text{if } t > 2\tau(K) \text{ and } n < 0; \\ 1, & \text{if } t < 2\tau(K) \text{ and } n > 0; \\ 0, & \text{otherwise.} \end{cases}
$$

$$
\begin{aligned}
\partial b_1 &= \rho_3 a_1 + U\rho_{123} a_2 \\
&\quad + U(b_2 + \rho_{123} e_1) \\
\partial(b_2 + \rho_{123} e_1) &= \rho_3 a_2 \\
\partial b_3 &= U\rho_1 a_2 \\
\partial a_1 &= \rho_2 b_3 + U a_2 \\
\partial a_3 &= U a_4 \\
\partial h_1 &= U h_2 + \rho_3 g_1 \\
&\quad + U\rho_{123}(e_1 + a_3) \\
\partial(h_2 + \rho_{123}) &= \rho_3 g_2 + U\rho_{123} e_2 \\
\partial f_1 &= U f_2 + U\rho_1 e_1 \\
\partial f_2 &= U\rho_1 e_2 \\
\partial g_1 &= U g_2 + \rho_2 f_1 \\
\partial g_2 &= \rho_2 f_2 \\
\partial e_1 &= U e_2 \\
\partial a_2 &= \partial a_4 = \partial e_2 = 0
\end{aligned}
$$

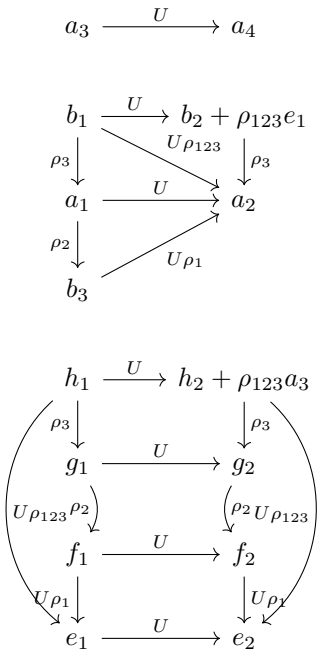


Figure 3.12: The type D module $\mathrm{CFD}^-(W(0;-2))$ after a change of basis
Replaced the generator b_2 in Figure 3.11 with $b_2 + \rho_{123} e_1$. Replaced the generator h_2 in Figure 3.11 with $h_2 + \rho_{123} a_3$.

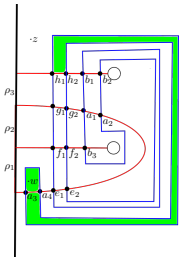
Proof. By the pairing theorem of bordered Floer homology, the knot Floer homology of the $-n$-clasped generalized Whitehead double is the boxed tensor product

$$\widehat{\mathrm{CFA}}(Y \setminus K) \boxtimes (\mathrm{CFD}^-(W(0;-n))).$$

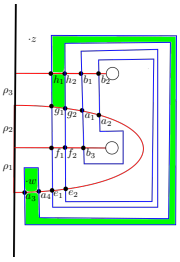
By Proposition 3.3.1, $\mathrm{CFK}^-(W(K,t;-n))$ contains a summand isomorphic to $\mathrm{CFK}^-(D_-(K,t))$. The component $\mathrm{CFK}^-(D_-(K,t))$ determines the invariant $\tau(W(K,t;-n))$ since the U-non-torsion elements must lie in this component. Therefore, the extra twistings in the clasp region of the generalized Whitehead double does not affect τ.

$$\tau(W(K,t;n)) = \begin{cases} \tau(D_+(K,t), & \text{if } n > 0; \\ \tau(D_-(K,t), & \text{if } n < 0. \end{cases}$$

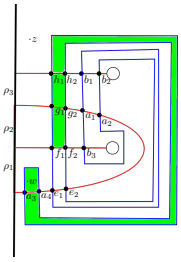
Using Theorem 1.4 of Hedden [5] and the mirroring property $\tau(-K) = -\tau(K)$ finishes the proof. □



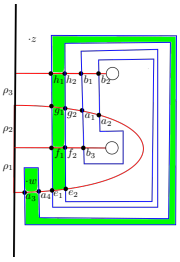
(a) $h_1 \to Uh_2$



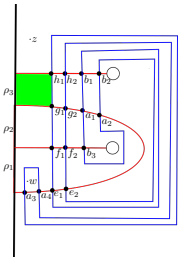
(b) $g_1 \to Ug_2$



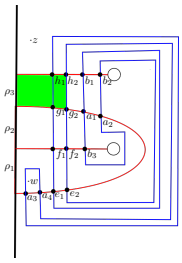
(c) $f_1 \to Uf_2$



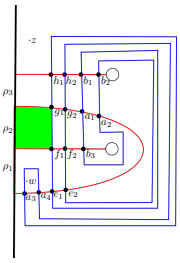
(d) $e_1 \to Ue_2$



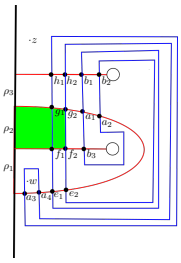
(e) $h_1 \to \rho_1 g_1$



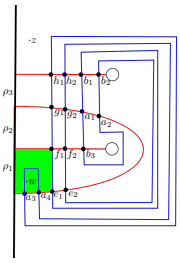
(f) $h_2 \to \rho_1 g_2$



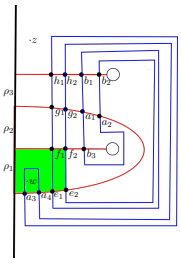
(g) $g_1 \to \rho_2 f_1$



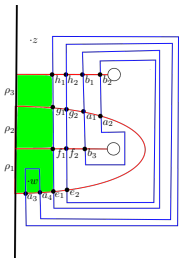
(h) $g_2 \to \rho_2 f_2$



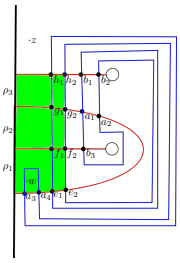
(i) $f_1 \to \rho_3 e_1$



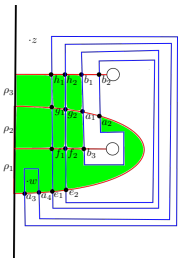
(j) $f_2 \to \rho_3 e_2$



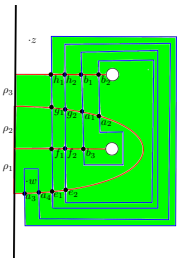
(k) $h_1 \to U\rho_{123}e_1$



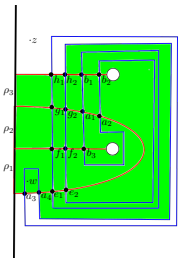
(l) $h_2 \to U\rho_{123}e_2$



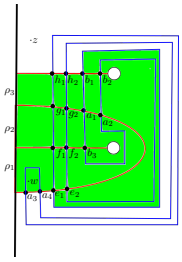
(m) $b_1 \to U\rho_{123}a_2$



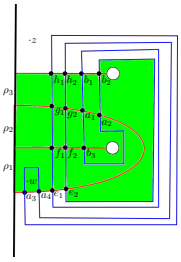
(n) $h_1 \to U\rho_{123}a_3$



(o) $h_2 \to U\rho_{123}a_4$



(p) $b_1 \to U\rho_{123}e_1$



(q) $b_2 \to U\rho_{123}e_2$

Figure 3.13: Counting immersed disks in $\mathrm{CFD}^-(W(0;-2))$ of a punctured solid torus with a -2-clasped Whitehead double pattern

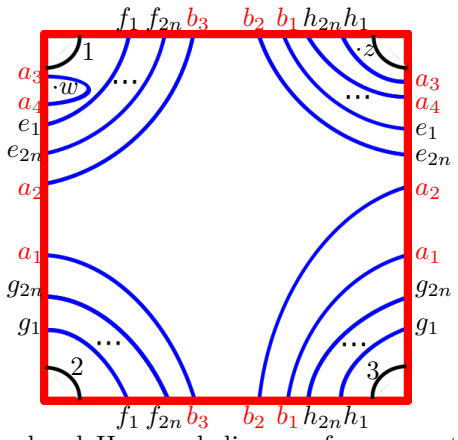
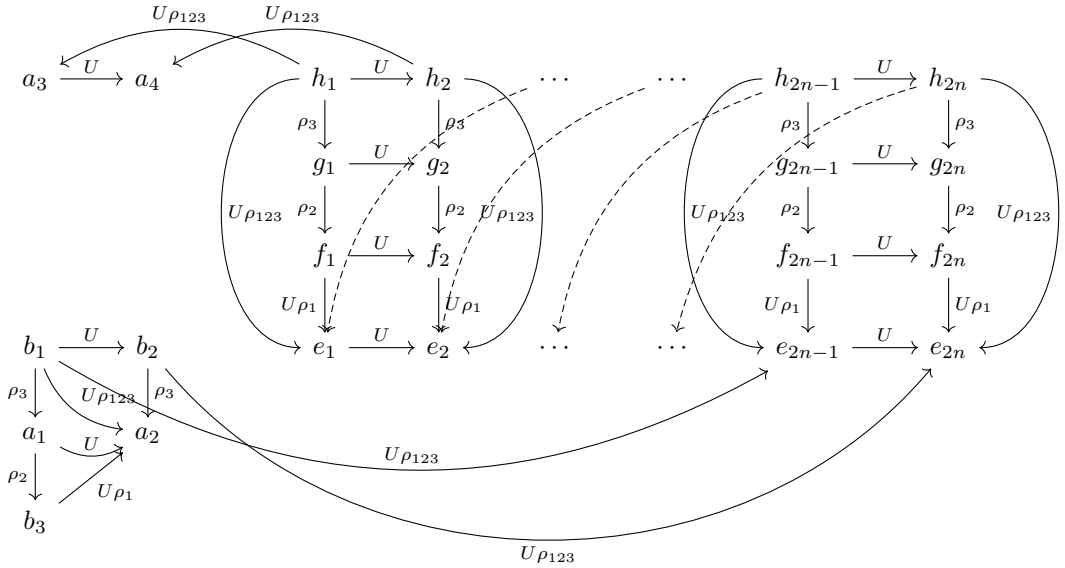
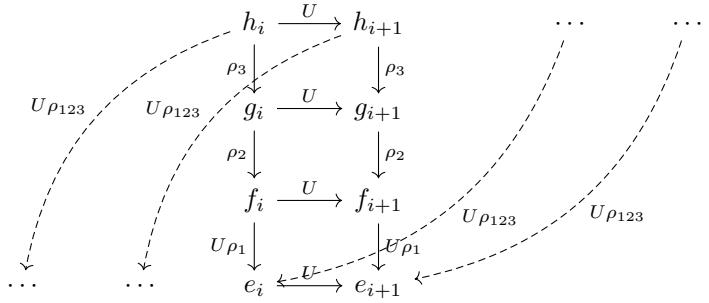


Figure 3.14: A doubly-pointed bordered Heegaard diagram for a punctured solid torus with the $-(n+1)-$clasped generalized Whitehead double pattern knot

The red generators correspond to the summand in CFD^- of the negatively-clasped Whitehead double pattern $W(0;-1)$. The black generators correspond to the new generators in CFD^- of the $(-n-1)-$clasped generalized Whitehead double.



where the dots indicate repetitions



for all i, an odd integer in $\{3,\dots,2n-3\}$.

Figure 3.15: The type D module $\mathrm{CFD}^-(W(0;-n))$

3.4 Further Directions

A longstanding conjecture states that a Whitehead double of a knot is slice if and only if the knot itself is slice. This conjecture can be extended to include generalized Whitehead doubles.

Conjecture 3.4.1. A generalized untwisted Whitehead double of K is slice if and only if K is slice.

Chapter 4

Knot Floer Homology of a Family of Knots μ_n in $S^3_t K$, $t >> 0$, and Concordance Invariants

4.1 Knot Floer Homology of a Family of Knots μ_n in $S^3_t K$, $t >> 0$, in terms of $\mathrm{CFK}^\infty(S^3, K)$

Recall the large integer surgery formula from Ozsváth and Szabó [23]. Let $(\Sigma_g, \alpha_1, \ldots, \alpha_g, \gamma_1, \ldots, \gamma_g, w, z)$ be a doubly-pointed Heegaard diagram for $\mathrm{CFK}^\infty(S^3, K)$, where the curve $\gamma_g = \mu$ is a meridian of the knot K, the curve α_g is a longitude for K, there is a single intersection point $\alpha_g \cap \gamma_g = x_0$, and the basepoints w and z lie on either side of γ_g. Let β be the set of curves in γ, with γ_g replaced by a longitude λ_t winding t times around μ. Label the unique intersection point $\lambda_t \cap \beta_g = \theta$. The Heegaard triple diagram $(\Sigma, \alpha, \beta, \gamma, w, z)$ represents a cobordism between S^3 and $S^3_t(K)$. See Figure 4.1.

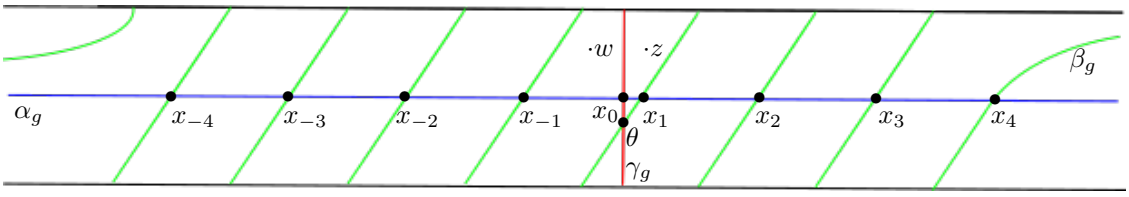


Figure 4.1: Local picture of the winding region of the Heegaard triple diagram $(\Sigma, \alpha, \beta, \gamma, w, z)$ for the cobordism between $S^3_t K$ and S^3

Let $C\{\max(i, j-m)\} = 0$ denote the subquotient complex of $\mathrm{CFK}^\infty(S^3, K)$ generated by triples $[x, i, j]$ with the i and j filtration levels satisfying the specified constraints. The chain map

$$\Phi_m : \widehat{\mathrm{CF}}(S^3_t(K), \mathfrak{s}_m) \to C\{\max(i, j-m) = 0\}$$

defined in [23] by

$$\Phi_m([x]) = \sum_{y \in T_\alpha \cap T_\gamma} \sum_{\{\psi \in \pi_2(x,\theta,y) \ \mid \ n_z(\psi) - n_w(\psi) = m - \mathcal{F}(y), \ \mu(\psi) = 0\}} [y, -n_w(\psi), m - n_z(\psi)]$$

induces an isomorphism of chain complexes.

We refine their formula to a filtered version. Consider the meridian μ_K of a knot K. μ_K naturally lies inside of the knot complement $S^3 \setminus K$ and the surgered manifold $S^3_t K$. In addition, there is a natural family of knots μ_n, where n is an integer, that lies inside $S^3 \setminus K$ and the surgered manifold $S^3_t K$. For $n = 1$, $\mu_1 = \mu_K$. The knot μ_n is homologically equivalent to $n \cdot [\mu_K]$ in $H_1(S^3_t(K))$, where μ_K is the meridian of K. See Figure 4.2 for a picture of the two-component link $K \cup \mu_n$.

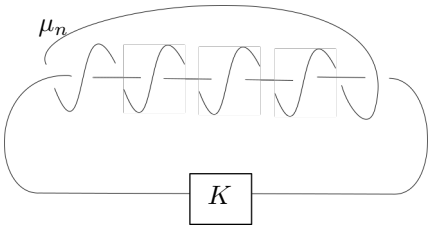


Figure 4.2: The two-component link μ_n and K for $n = 4$

For all $n \geq 1$ we have a natural $(n+1)$-step algebraic filtration $\mathcal{G}$ on $C\{\max(i, j-m) = 0\}$:

$$\begin{aligned} 0 \subseteq C\{i < -n+1, j = m\} &\subseteq C\{i < -n+2, j = m\} \\ &\cdots \subseteq C\{i < 0, j = m\} \\ &\subseteq C\{\max(i, j-m) = 0\}. \end{aligned}$$

This corresponds to a relative $\mathbb{Z}$-filtration on $\widehat{\mathrm{CF}}(S^3_t(K), \mathfrak{s}_m)$ induced by a knot $\mu_n \in S^3_t(K)$:

Theorem 4.1.1. *The filtered chain homotopy type of the $(n+1)$ step filtered complex $\mathcal{G}$ is filtered chain homotopy equivalent to that of $\widehat{CF}(S^3_t(K), \mathfrak{s}_m)$ with filtration induced by the knot $\mu_n \in S^3_t K$. Here, t is any integer greater than $2g(K) - 1$, $n < t/2$, and m is any integer.*

Proof. Place an extra basepoint $z' = z_n$ so that it is n "steps" away from the basepoint w in the Heegaard triple diagram representing the cobordism between S^3 and $S^3_t(K)$ used in [23]. The knot represented by the doubly-pointed Heegaard diagram $(\Sigma, \alpha, \gamma, w, z_n)$ is $\mu_n \sim n \cdot \mu_K$ in $S^3_t(K)$.

Fix a Spin^c structure $\mathfrak{s}_m$ where $m \in \mathbb{Z}$. For t (the surgery coefficient) sufficiently large, any generator $x' \in T_\alpha \cap T_\beta$ representing Spin^c structure $\mathfrak{s}_m$ is supported in the winding region. In this case, there is a uniquely determined $x \in T_\alpha \cap T_\gamma$ and a canonical small triangle $\psi \in \pi_2(x, \theta, x')$.

If $x' \in T_\alpha \cap T_\beta$ is a generator representing Spin^c structure $\mathfrak{s}_m$ with $k = n_z(\psi) \geq 0$ (so $n_w(\psi) = 0$), then the α_g component of x' is x_{k+1} and lies $k+1$ units to the left of x_0 in Figure 4.3, where $\psi \in \pi_2(x, \theta, x')$ is the canonical small triangle. In this case, Φ_m maps x' to $C\{i = 0, j \leq m\}$. On the other hand, if x' is a generator with $n_z(\psi) = 0$ and $l = n_w(\psi) > 0$, then the α_g component of x' is x_{-l} and lies l steps to the right of x_0 in Figure 4.3. In this case, Φ_m maps x' to $C\{i \leq -l, j = m\} \subset C\{i < 0, j = m\}$.

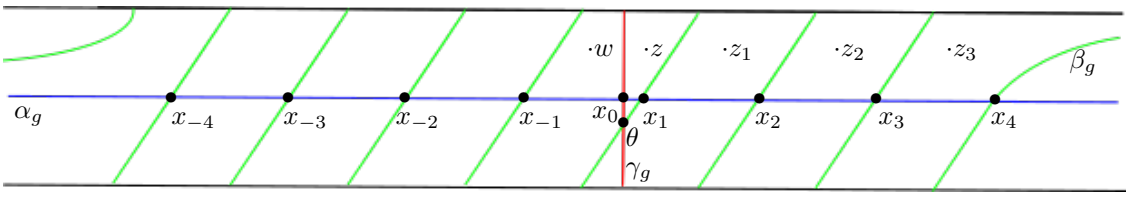


Figure 4.3: Local picture of the winding region of the Heegaard triple diagram $(\Sigma, \alpha, \beta, \gamma, w, z_n)$ for the cobordism between $S^3_t K$ and S^3
The basepoint z_n is n "steps" away from the basepoint w in the Heegaard triple diagram representing the 2-handle addition cobordism. Here we depict the basepoint z_n for $n = 1$, 2, and 3.

The relative $\mathbb{Z}$-filtration (the *Alexander* filtration) A' induced by the knot represented by $(\Sigma, \alpha, \gamma, w, z_n)$ is given by $A'_n(x') - A'_n(y') = n_{z_n}(\phi) - n_w(\phi)$ where $\phi \in \pi_2(x', y')$.

The filtration level of the generators x', y' with α_g component on the left of x_0 are all equal because disks $\phi \in \pi_2(x', y')$ with $n_w(\phi) = 0$ necessarily have $n_{z_n}(\phi) = 0$.

The filtration difference between the generators with α_g component on the left of x_0 and the generators with α_g component equal to x_{-1} (i.e. one step to the right of x_0) is 1. That is, if x' has α_g component on the left of x_0 and y' has α_g component one step to the right of x_0 and $\phi \in \pi_2(x', y')$ with $n_w(\phi) = 0$,

$$A'_n(x') - A'_n(y') = n_{z_n}(\phi) - n_w(\phi) = 1.$$

All generators with α_g component lying n steps or more to the right of x_0 belong in the same Alexander filtration A'. This is true because if $n_w(\phi) = 0$ then $n_{z_n}(\phi) = 0$ where ϕ is a Whitney disk connecting two such generators. If $0 < i < n$, a generator x' with α_g component x_{-i}, that is i steps to the right of x_0, lies

in filtration level that is i lower than those generators y' with α_g component on the left of x_0.

$$A'_n(y') - A'_n(x') = n_{z_n}(\phi) - n_w(\phi) = i.$$

This completes the description of the knot Floer filtered chain complex of $(S^3_t(K), \mu_n)$ in terms of the complex $\mathrm{CFK}^\infty(S^3, K)$. □

Remark 4.1.2. We described the filtration induced by μ_n on the hat version of Heegaard Floer homology $\widehat{\mathrm{HF}}(S^3_t(K))$ of large integer surgery along K. Similarly, we can describe the filtrations induced by μ_n on the infinity, plus, and minus versions of the Heegaard Floer homology of $S^3_t K$. The Alexander filtration levels induced by μ_n on $\mathrm{CFK}^\infty(Y_t(K), \mu_n, \mathfrak{s}_m)$ are obtained from the Alexander filtration on $\widehat{\mathrm{CFK}}(Y_t(K), \mu_n, \mathfrak{s}_m)$ by using the relation $A(U \cdot x) = A(x) - 1$. Up to a grading shift, the pth filtration level of $\mathrm{CFK}^\infty(S^3_t(K), \mu_n, \mathfrak{s}_m)$ is described in terms of the original $\mathbb{Z} \oplus \mathbb{Z}-$filtered knot Floer homology $\mathrm{CFK}^\infty(S^3, K)$ as

$$\max(i, j - m - n) = p.$$

As evident, each filtration level p of $\mathrm{CFK}^\infty(S^3_t(K), \mu_n, \mathfrak{s}_m)$ is a "hook" shaped region in $\mathrm{CFK}^\infty(S^3, K)$.

Remark 4.1.3. For large integer surgery and sufficiently large n (for $n > g(K)$, corresponding to μ_n), the corners of the hooks of all the filtration levels of $\mathrm{CFK}^\infty(S^3_t K, \mu_n, \mathfrak{s}_m)$ lie above the thick diagonal along which $\mathrm{CFK}^\infty(Y, K)$ is supported. This means that the Alexander filtration induced by μ_n (for $n > g(K)$) on $\mathrm{CFK}^\infty(S^3_t(K), \mu_n, \mathfrak{s}_m)$ coincides with the algebraic i-filtration on $\mathrm{CFK}^\infty(S^3, K)$ under the correspondence given by Theorem 4.1.1.

Since the algebraic i-filtration is used to define concordance invariants (see the next section), this family of knots μ_n is directly related to concordance information of K.

4.2 Background on the concordance invariants ϵ and a_1

Recall the definition of the concordance invariant ϵ in [6]. Let N be a sufficiently large integer. Consider the map

$$F_s : \widehat{\mathrm{HF}}(S^3) \to \widehat{\mathrm{HF}}(S^3_{-N}(K), [s]),$$

induced by the two-handle cobordism W^4_{-N}. Here, $[s]$ denotes the restriction to $S^3_{-N}(K)$ of the Spin^c structure $\mathfrak{s}_s$ over W^4_{-N} with the property that

$$\langle c_1(\mathfrak{s}_s), [\widehat{F}] \rangle - N = 2s,$$

where $|s| \leq \frac{N}{2}$ and $\widehat{F}$ denotes the capped off Seifert surface in the four-manifold. We also consider the map

$$G_s : \widehat{\mathrm{HF}}(S^3_N(K), [s]) \to \widehat{\mathrm{HF}}(S^3),$$

induced by the two-handle cobordism $-W^4_N$.

The maps F_s and G_s can be defined algebraically by studying certain natural maps on subquotient complexes of $\mathrm{CFK}^\infty(K)$, as in [23]. The map F_s is induced by the chain map

$$C\{i = 0\} \to C\{\min(i, j - s) = 0\}$$

consisting of quotienting by $C\{i = 0, j < s\}$ followed by the inclusion. Similarly, the map G_s is induced by the chain map

$$C\{\max(i, j - s) = 0\} \to C\{i = 0\}$$

consisting of quotienting by $C\{i < 0, j = s\}$ followed by the inclusion.

Definition 4.2.1 (Hom [6], [7])**.** The invariant ϵ is defined in terms of F_τ and G_τ as follows:

- $\epsilon = 1$ if F_τ is trivial (in which case G_τ is necessarily non-trivial).
- $\epsilon = -1$ if G_τ is trivial (in which case F_τ is necessarily non-trivial).
- $\epsilon = 0$ if F_τ and G_τ are both non-trivial.

In [7], Hom defines a refinement of ϵ for knots with $\epsilon(K) = 1$: a concordance invariant $a_1(K)$.

Definition 4.2.2 (Hom [7])**.** If $\epsilon(K) = 1$ (F_τ is trivial), define

$$a_1(K) = \min\{s \mid H_s : H_*(C\{i = 0\}) \to H_*(C\{\min(i, j - \tau) = 0, i \leq s\}) \text{ is trivial}\}$$

In the next section, we extend this definition to all knots, and call this refinement $\tilde{\epsilon}$.

4.3 A refinement of ϵ

Consider the maps

$$G_{-n,\tau} : C\{\max(i, j - \tau) = 0, i \geq -n\} \to C\{i = 0\}$$

$$F_{n,\tau} : C\{i = 0\} \to C\{\min(i, j - \tau) = 0, i \leq n\}$$

Definition 4.3.1. Given a knot K inside S^3, define $\tilde{\epsilon}$ as follows:

$$\tilde{\epsilon}(K) = \begin{cases} \max\{-n \mid G_{-n,\tau} \text{ is trivial on homology}\}\,, & \text{if } \epsilon(K) = -1; \\ 0, & \text{if } \epsilon(K) = 0; \\ \min\{n \mid F_{n,\tau} \text{ is trivial on homology}\}\,, & \text{if } \epsilon(K) = 1. \end{cases}$$

Note that $\tilde{\epsilon}$ only depends on the doubly-filtered chain homotopy type of the knot Floer chain complex $CFK^\infty(K)$, so it is a knot invariant.

Remark 4.3.2. When $\epsilon = 1$, the definition of $\tilde{\epsilon}$ agrees with the invariant "$a_1(K)$" defined in Lemma 6.1 in [7], and as remarked in [7], $\tilde{\epsilon}$ measures the "length" of the horizontal differential hitting the special class generating the vertical homology of $\widehat{\mathrm{CF}}(S^3)$. Similarly, when $\epsilon = -1$, $\tilde{\epsilon}$ measures the "length" of the horizontal differential coming out of the special class generating the vertical homology of $\widehat{\mathrm{CF}}(S^3)$.

According to Theorem 4.1.1, an equivalent definition of $\tilde{\epsilon}$ is:

Definition 4.3.3. $\tilde{\epsilon}(K) =$

$$\begin{cases} \max\left\{m \mid \frac{\widehat{\mathrm{CFK}}(S^3_N K,\ s_\tau, \mu_n)}{\mathcal{F}(\mu_n, \mathrm{top}-1-m)} \to \widehat{\mathrm{CF}}(S^3) \text{ is trivial on } H_*\right\}, & \text{if } \epsilon(K) = -1; \\ 0, & \text{if } \epsilon(K) = 0; \\ \min\left\{m \mid \widehat{\mathrm{CF}}(S^3) \to \mathcal{F}'(\mu_n, \mathrm{bottom} + m) \subset \widehat{\mathrm{CFK}}(S^3_{-N} K, \mathfrak{s}_\tau, \mu_n) \text{ is trivial on } H_*\right\}, & \text{if } \epsilon(K) = 1; \end{cases}$$

where n, N are sufficiently large, $\mathcal{F}(\mu_n, \mathrm{top} - m)$ denotes the filtered subcomplex of $\widehat{\mathrm{CFK}}(S^3_N K, \mathfrak{s}_\tau, \mu_n)$ consisting of generators with Alexander filtration $\leq \mathrm{top} - m$, top is the highest Alexander filtration level of $\widehat{\mathrm{CFK}}(S^3_N K, \mathfrak{s}_\tau, \mu_n)$, $\mathcal{F}'(\mu_n, \mathrm{bottom} + m) \subset \widehat{\mathrm{CFK}}(S^3_{-N} K, \mathfrak{s}_\tau, \mu_n)$ denotes the subcomplex consisting of generators with Alexander filtration $\leq \mathrm{bottom} + m$, and bottom is the lowest Alexander filtration level of $\widehat{\mathrm{CFK}}(S^3_{-N} K, \mathfrak{s}_\tau, \mu_n)$.

Proposition 4.3.4. *The invariant $\tilde{\epsilon}$ is a concordance invariant.*

Proof. Suppose K_1 and K_2 are concordant knots, i.e. $K_1 \# \overline{K_2}$ is slice. Then $\epsilon(K_1 \# \overline{K_2}) = 0$. By Proposition 3.11 in [8], we may find a basis for $\mathrm{CFK}^\infty(K_1 \# \overline{K_2})$ with a distinguished element x that generates the homology $\mathrm{HFK}^\infty(K_1 \# \overline{K_2})$ and splits off as a direct summand of $\mathrm{CFK}^\infty(K_1 \# \overline{K_2})$. Similarly, we can find a basis for $\mathrm{CFK}^\infty(K_2 \# \overline{K_2})$ with a distinguished element y with the same properties. Then to compute $\tilde{\epsilon}(K_2 \# K_1 \# \overline{K_2})$, by the Kunneth principle [23] we can consider either chain complex:

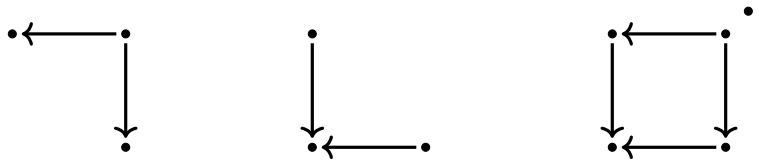
$$\mathrm{CFK}^\infty(K_1 \# \overline{K_2}) \otimes_{\mathbb{Z}[U,U^{-1}]} \mathrm{CFK}^\infty(K_2) \quad \text{or} \quad \mathrm{CFK}^\infty(K_1) \otimes_{\mathbb{Z}[U,U^{-1}]} \mathrm{CFK}^\infty(K_2 \# \overline{K_2}).$$

Using the special bases from above, the relevant summands to $\tilde{\epsilon}$ are

$$\{x\} \otimes \mathrm{CFK}^\infty(K_2) \quad \text{or} \quad \mathrm{CFK}^\infty(K_1) \otimes \{y\}.$$

Thus, $\tilde{\epsilon}(K_2) = \tilde{\epsilon}(K_2 \# K_1 \# \overline{K_2}) = \tilde{\epsilon}(K_1)$. □

Example 4.3.5. We compute $\tilde{\epsilon}$ for the left-handed and right-handed trefoils and the figure eight knot. Knot Floer chain complexes CFK^∞ of these knots are given in Figure 4.4.



(a) $\tilde{\epsilon}(K) = 1$ (b) $\tilde{\epsilon}(K) = -1$ (c) $\tilde{\epsilon}(K) = 0$

Figure 4.4: The generators for $CFK^\infty(K)$, over $\mathbb{F}[U, U^{-1}]$, for different knots K. Above left, K is the right-handed trefoil, which has $\tilde{\epsilon}(K) = 1$. Center, K is the left-handed trefoil, which has $\tilde{\epsilon}(K) = -1$. Right, K is the figure 8 knot, which has $\tilde{\epsilon}(K) = 0$.

Example 4.3.6 (Homologically thin knots)**.** Model complexes for CFK^∞ of homologically thin knots are studied in [30]. Petkova shows that if $\tau(K) = n$, the model complex contains a direct summand isomorphic to

$$\mathrm{CFK}^\infty(T_{2,2n+1}) \text{ if } n > 0 \quad \text{and} \quad \mathrm{CFK}^\infty(T_{2,2n-1}) \text{ if } n < 0.$$

This summand supports $H_*(\mathrm{CFK}^\infty(K))$ and thus determines the value of $\tilde{\epsilon}$. It is easy to see from the complex that $\tilde{\epsilon} = \mathrm{sgn}(\tau)$.

Proposition 4.3.7. *The following are properties of $\tilde{\epsilon}(K)$:*

(1) If K is smoothly slice, then $\tilde{\epsilon}(K) = 0$.

(2) $\mathrm{sgn}(\tilde{\epsilon}(K)) = \mathrm{sgn}(\epsilon(K))$. In particular, $\tilde{\epsilon}(K) = 0$ implies $\epsilon(K) = 0$ and $\tau(K) = 0$.

(3) $\tilde{\epsilon}(K) = -\tilde{\epsilon}(\overline{K})$.

(4) If $\tilde{\epsilon}(K) = 0$, then $\tilde{\epsilon}(K \# K') = \tilde{\epsilon}(K')$.

Proof of (1). If K is smoothly slice, then $\epsilon(K) = 0$; therefore, $\tilde{\epsilon}(K) = 0$. □

Proof of (2). By construction, if $\tilde{\epsilon}(K) > 0$, then $\epsilon(K) = 1$; if $\tilde{\epsilon}(K) < 0$, then $\epsilon(K) = -1$.

If $\tilde{\epsilon}(K) = 0$, we show that $\epsilon(K) = 0$. Suppose $\epsilon(K) = -1$. Then the vanishing of

$$\tilde{\epsilon}(K) = \max\{n \mid G_{n,\tau} \text{ is trivial on homology}\}$$

implies that the map $G_{0,\tau} : C\{i = 0, j \leq \tau\} \to C\{i = 0\}$ is trivial on homology, which contradicts the definition of τ. Similarly, $\epsilon(K) \neq 1$ if $\tilde{\epsilon}(K) = 0$.

Finally, according to [6], $\epsilon(K) = 0$ implies that $\tau(K) = 0$. □

Proof of (3). The symmetry properties of CFK^∞ of Section 3.5 in [23] imply that $\tilde{\epsilon}(K) = -\tilde{\epsilon}(\overline{K})$. □

Proof of (4). If $\tilde{\epsilon}(K) = 0$, $\epsilon(K) = 0$. By Lemma 3.3 from [6], we may find a basis for $\mathrm{CFK}^\infty(K)$ with a distinguished element x which is the generator of both vertical and horizontal homology. Then $\tilde{\epsilon}(K\#K')$ can be computed from $\{x\} \otimes \mathrm{CFK}^\infty(K')$. □

In fact, we can extend Proposition 4.3.7(4) to describe the behavior of $\tilde{\epsilon}$ under connect sum in many (but not all) cases.

Proposition 4.3.8.

(1) If $\tilde{\epsilon}(K_1) > 0$ *and* $\tilde{\epsilon}(K_2) < 0$ *and* $\tilde{\epsilon}(K_1) + \tilde{\epsilon}(K_2) < 0$, *then* $\tilde{\epsilon}(K_1\#K_2) = \tilde{\epsilon}(K_1)$.

(2) If $\tilde{\epsilon}(K_1) > 0$ *and* $\tilde{\epsilon}(K_2) < 0$ *and* $\tilde{\epsilon}(K_1) + \tilde{\epsilon}(K_2) > 0$, *then* $\tilde{\epsilon}(K_1\#K_2) = \tilde{\epsilon}(K_2)$.

(3) If $\tilde{\epsilon}(K_1) > 0$ *and* $\tilde{\epsilon}(K_2) > 0$, *then* $\tilde{\epsilon}(K_1\#K_2) = \min(\tilde{\epsilon}(K_1), \tilde{\epsilon}(K_2))$.

(4) If $\tilde{\epsilon}(K_1) < 0$ *and* $\tilde{\epsilon}(K_2) < 0$, *then* $\tilde{\epsilon}(K_1\#K_2) = \max(\tilde{\epsilon}(K_1), \tilde{\epsilon}(K_2))$.

Proof. Note that we use $-K$ to denote the mirror of a knot K.

(1) See the proof of Lemma 6.3 of [7].

(2) The mirrors $-K_1$ and $-K_2$ satisfy the hypothesis of (1), so

$$\tilde{\epsilon}(-K_1\# - K_2) = \tilde{\epsilon}(-K_2).$$

Apply the symmetry property of $\tilde{\epsilon}$ under mirroring (4.3.7):

$$-\tilde{\epsilon}(K_1\#K_2) = -\tilde{\epsilon}(K_2)$$

as desired.

(3) By Lemma 6.2 of [7], there exists a basis $\{x_i\}$ over $\mathbb{F}[U, U^{-1}]$ for $\mathrm{CFK}^\infty(K_1)$ with basis elements x_0 and x_1 with the property that

1. There is a horizontal arrow of length $\tilde{\epsilon}$ from x_1 to x_0.
2. There are no other horizontal arrows or vertical arrows to or from x_0.
3. There are no other horizontal arrows to or from x_1.

Similarly, we may find a basis $\{y_i\}$ over $\mathbb{F}[U, U^{-1}]$ for $\mathrm{CFK}^\infty(K_2)$ with basis elements y_0 and y_1 with the above properties. Without loss of generality, assume that $\tilde{\epsilon}(K_1) \leq \tilde{\epsilon}(K_2)$.

Notice x_0y_0 generates the vertical homology $H_*(C(\{i = 0\}))$ of $\mathrm{CFK}^\infty(K_1\#K_2)$. Let $\tau = \tau(K_1\#K_2)$. Consider the subquotient complex

$$A = C\{\min(i, j - \tau) = 0\}.$$

There is a direct summand of A consisting of the generators x_0y_0, x_0y_1, x_1y_0, and x_1y_1, and four horizontal arrows as shown in Figure 4.5. The arrow x_1y_0 to x_0y_0 has length $\tilde{\epsilon}(K_1)$. Clearly, $\epsilon(K_1\#K_2) = 1$ and $\tilde{\epsilon}(K_1\#K_2) = \tilde{\epsilon}(K_1)$.

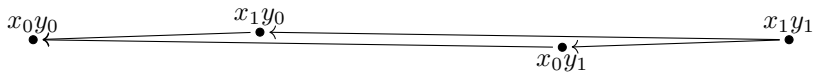


Figure 4.5: A direct summand of $A = C\{\min(i, j - \tau) = 0\}$ in Proposition 4.3.8(3)
This is the summand that is relevant for computing $\tilde{\epsilon}$, as it contains the generator x_0y_0 of vertical homology $H_*(C\{i = 0\})$.

(4) The mirrors $-K_1$ and $-K_2$ satisfy the hypothesis of (3). So

$$\begin{aligned} -\tilde{\epsilon}(K_1\#K_2) = \tilde{\epsilon}(-K_1\# - K_2) = \min(\tilde{\epsilon}(-K_1), \tilde{\epsilon}(-K_2)) &= \min(-\tilde{\epsilon}(K_1), -\tilde{\epsilon}(K_2)) \\ &= -\max(\tilde{\epsilon}(K_1), \tilde{\epsilon}(K_2)). \end{aligned}$$

□

Proposition 4.3.8 can be rewritten as the following.

Proposition 4.3.9. *If $\tilde{\epsilon}(K_1) \neq 0$ and $\tilde{\epsilon}(K_2) \neq 0$:*

(1) If $\tilde{\epsilon}(K_1) + \tilde{\epsilon}(K_2) < 0$, then $\tilde{\epsilon}(K_1\#K_2) = \max(\tilde{\epsilon}(K_1), \tilde{\epsilon}(K_2))$.

(2) If $\tilde{\epsilon}(K_1) + \tilde{\epsilon}(K_2) > 0$, then $\tilde{\epsilon}(K_1\#K_2) = \min(\tilde{\epsilon}(K_1), \tilde{\epsilon}(K_2))$.

Remark 4.3.10. If $\tilde{\epsilon}(K) \neq 0$ and $\tilde{\epsilon}(K') \neq 0$, and $\tilde{\epsilon}(K) + \tilde{\epsilon}(K') = 0$, then the behavior of $\tilde{\epsilon}(K\#K')$ is unpredictable. The next two examples illustrate this feature.

Example 4.3.11. The connect sum of any knot K with the reverse of its mirror $-K$, i.e. the inverse of K in the concordance group $\mathcal{C}$, has vanishing $\tilde{\epsilon}(K\# - K) = 0$.

Example 4.3.12. The full knot Floer chain complexes CFK^∞ of the mirror $-T_{2,3;2,5}$ of the $(2,5)$-cable of the torus knot $T_{2,3}$, the torus knot $T_{2,9}$, and the connect sum $-T_{2,3;2,5}\#T_{2,9}$ are described in [11]. It is easy to see that $\tilde{\epsilon}(-T_{2,3;2,5}) = -1$, $\tilde{\epsilon}(T_{2,9}) = 1$, and $\tilde{\epsilon}(-T_{2,3;2,5}\#T_{2,9}) = -1$.

We provide more examples of knots with computable $\tilde{\epsilon}$.

Example 4.3.13. In [10] Hom produces the relevant summand of CFK^∞ for computing ϵ and hence $\tilde{\epsilon}$ for the knot $T_{4,5}\# - T_{2,3;2,5}$. It is easy to see that $\tilde{\epsilon}(T_{4,5}\# - T_{2,3;2,5}) = 2$.

Example 4.3.14. The Conway knot $C_{2,1}$ has $\tilde{\epsilon}(C_{2,1}) = 0$. According to [29], the knot Floer chain complex $\mathrm{CFK}^\infty(C_{2,1})$ is generated as a $\mathbb{F}[U, U^{-1}]-$module by a single isolated $\mathbb{F}$ at the origin plus a collection of null-homologous "boxes".

Example 4.3.15. The knot Floer chain complex of an L-space knot is a given by Theorem 2.1 in [21]. If K is an L-space knot, with Alexander polynomial

$$\Delta_K(t) = \sum_{i=0}^{k} (-1)^i t^{n_i},$$

where $n_0 > n_1 > \cdots > n_k$, then $\tilde{\epsilon}(K) = n_0 - n_1$ by Lemma 6.5 [7].

Example 4.3.16. There exist knots with τ and ν^+ arbitrarily larger than $\tilde{\epsilon}$. Torus knots have $\tau(T_{p,q}) = \frac{(p-1)(q-1)}{2}$ equal to their $4-$ball genus $g_4(T_{p,q})$. In Lemma 6.7 of [7], Hom shows that the knots $T_{p,p+1}$ have $\tilde{\epsilon}(T_{p,p+1}) = 1$.

4.4 Further Directions

4.4.1 Properties of $\tilde{\epsilon}$

Question 4.4.1. The concordance invariants τ, ν, ν^+, and $\nu^{+'}$ give lower bounds on the four-ball genus of a knot. It is natural to ask whether the absolute value of $\tilde{\epsilon}(K)$ also provides a lower bound on the four-ball genus $g_4(K)$? We conjecture that the answer is affirmative.

Question 4.4.2. Let K_+ be a knot in S^3, and let K_- be a knot obtained from K_+ by changing one positive crossing to a negative crossing. The invariants τ and ν^+ satisfy similar properties with respect to crossing changes:

$$\tau(K_+) - 1 \leq \tau(K_-) \leq \tau(K_+)$$

and

$$\nu^+(K_+) - 1 \leq \nu^+(K_-) \leq \nu^+(K_+),$$

where the first relation is due to [22] and the second relation is due to [1]. Does $\tilde{\epsilon}$ also transform predictably under crossing changes?

Question 4.4.3. Let $K_{p,q}$ denote the (p,q)-cable of a knot K. In [6], Hom computes the invariants $\epsilon(K_{p,q})$ and $\tau(K_{p,q})$ in terms of p, q, $\epsilon(K)$ and $\tau(K)$. Is $\tilde{\epsilon}(K_{p,q})$ also determined by the same data, i.e. p, q, $\epsilon(K)$ and $\tau(K)$?

Question 4.4.4. In [11] Hom and Wu provide a family of knots whose ν^+ invariant grows arbitrarily larger than τ. Does this family of knots also exhibit the property that $\tilde{\epsilon}$ grows arbitrarily larger than τ? In general, can $\tilde{\epsilon}(K)$ be arbitrarily larger than $\tau(K)$?

4.4.2 Construct an HF^+ version of ϵ and $\tilde{\epsilon}$

A future research project is to investigate a way to use HF^+ to extract a concordance invariant analogous to ϵ and $\tilde{\epsilon}$. The invariant ϵ is defined using the concordance invariants ν and ν', which are defined using cobordism maps on $\widehat{\mathrm{HF}}$. We ask whether their "plus" counterparts ν^+ and $\nu^{+'}$, defined using cobordism maps on HF^+, can be similarly employed to construct a concordance invariant ϵ^+.

4.4.3 Generalizing the two-component link used in the construction of $\tilde{\epsilon}$

Question 4.4.5. Can we generalize $\tilde{\epsilon}$ by replacing $\mu_n \cup K$ by a two-component link $k_2 \cup K$ in order to achieve a concordance invariant of K?

Chapter 5

Truncated Heegaard Floer Homology and Concordance Invariants

In this chapter we construct a sequence of knot invariants $\nu_n(K)$, where $n \in \mathbb{Z}$, with the following properties:

- $\nu_n(K)$ is a concordance invariant.
- $\nu_1(K) = \nu(K)$ and $\nu_{-1}(K) = \nu'(K)$.
- $\nu_n(K) \leq \nu_{n+1}(K)$.
- For sufficiently large positive n, $\nu_n(K) = \nu^+(K)$.
- For sufficiently large negative n, $\nu_n(K) = \nu^{+'}(K)$.

The construction of the concordance invariants ν_n uses truncated Heegaard Floer homology, which we review below.

5.1 Truncated Heegaard Floer homology

A *truncated* version HF^n of Heegaard Floer Homology is described in [20, 27]. $\mathrm{HF}^n(Y, \mathfrak{s})$ is the homology of the kernel $\mathrm{CF}^n(Y, \mathfrak{s})$ of the multiplication map

$$U^n : \mathrm{CF}^+(Y, \mathfrak{s}) \to \mathrm{CF}^+(Y, \mathfrak{s})$$

where $n > 0$. The short exact sequence

$$0 \longrightarrow \mathrm{CF}^n(Y, \mathfrak{s}) \longrightarrow \mathrm{CF}^+(Y, \mathfrak{s}) \xrightarrow{U^n} \mathrm{CF}^+(Y, \mathfrak{s}) \longrightarrow 0$$

induces a long exact sequence

$$\cdots \longrightarrow \mathrm{HF}^n(Y, \mathfrak{s}) \longrightarrow \mathrm{HF}^+(Y, \mathfrak{s}) \longrightarrow \mathrm{HF}^+(Y, \mathfrak{s}) \longrightarrow \cdots$$

A four-dimensional cobordism equipped with a Spin^c structure between two three-manifolds induces a map on the Heegaard Floer homology groups [26]. In particular, for a knot K in S^3, the 2-handle attachment cobordism from a surgered manifold $S^3_N(K)$ to S^3 induces maps:

$$\hat{f}_s : \widehat{\mathrm{HF}}(S^3_N(K), \mathfrak{s}_s) \to \widehat{\mathrm{HF}}(S^3)$$

$$f^+_s : \mathrm{HF}^+(S^3_N(K), \mathfrak{s}_s) \to \mathrm{HF}^+(S^3)$$

where $\mathfrak{s}_s$ denotes the restriction to $S^3_N(K)$ of a certain Spin^c structure on the corresponding 2-handle cobordism. These cobordism maps on $\widehat{\mathrm{HF}}$ and HF^+ play a key role in defining concordance invariants such as τ, ν, ν^+ and ϵ. A 2-handle cobordism $(W, \mathfrak{s})$ also induces a map on the truncated Floer chain complexes $F^n_{W,\mathfrak{s}} : \mathrm{CF}^n(S^3_N K, \mathfrak{s}_s) \to \mathrm{CF}^n(S^3)$ and truncated Floer homologies

$$f^n_s : \mathrm{HF}^n(S^3_N K, \mathfrak{s}_s) \to \mathrm{HF}^n(S^3).$$

The *large integer surgery formula* of Ozsváth-Szabó [23] describes the Heegaard Floer chain complex of $S^3_N(K)$ in terms of the knot Floer chain complex $\mathrm{CFK}^\infty(S^3, K)$ of K. This formula leads to an interpretation of the cobordism maps $\hat{f}_s$, f^+_s, and f^n_s in terms of maps on subquotient complexes of $\mathrm{CFK}^\infty(S^3, K)$. Ozsváth and Szabó define a holomorphic triangle counting map that induces an isomorphism of chain complexes between suitably defined subquotient complexes of $\mathrm{CFK}^\infty(S^3, K)$ and the Heegaard Floer chain complexes for $S^3_N(K)$ for sufficiently large N. Their proof relies on a particular Heegaard diagram for the 2-handle cobordism where the generators and holomorphic disks in the chain complex for (S^3, K) correspond directly to those in the chain complex for $S^3_N(K)$. We extend the large integer surgery formula of Ozsváth-Szabó to truncated Heegaard Floer homology HF^n. As in their proof, we use a particular Heegaard diagram for the 2-handle cobordism and a holomorphic triangle counting map to get the desired isomorphism.

5.2 A sequence of concordance invariants ν_n

Definition 5.2.1. For positive n, define

$$\nu_n(K) = \min\{s \in \mathbb{Z} \mid F^n_{W,s} : \mathrm{CF}^n(S^3_N(K), s) \to \mathrm{CF}^n(S^3) \text{ induces a surjection on homology}\},$$

and for negative n, define

$$\nu_n(K) = \max\{s \in \mathbb{Z} \mid F^{-n}_{W,s} : \mathrm{CF}^{-n}(S^3) \to \mathrm{CF}^{-n}(S^3_{-N}(K), s) \text{ induces an injection on homology}\},$$

where N is sufficiently large so that the large integer surgery formula holds. Define $\nu_0(K) = \tau$.

Remark 5.2.2. For $n = \pm 1$, these invariants are already known as: $\nu_1 = \nu$ and $\nu_{-1} = \nu'$.

Proposition 5.2.3. *$\nu_n(K)$ is a concordance invariant.*

Proof. Suppose K_1 is concordant to K_2. Then $S^3_N(K_1)$ is homology cobordant to $S^3_N(K_2)$. This implies that there exists a (smooth, connected, oriented) cobordism W from $S^3_N(K_1)$ to $S^3_N(K_2)$ with $H_i(W, \mathbb{Q}) = 0$ for $i = 1, 2$.

The map

$$\mathrm{HF}^n(S^3_N(K_1), s) \to \mathrm{HF}^n(S^3)$$

induced by the cobordism obtained by adding a two-handle along K_1 factors through $\mathrm{HF}^n(S^3_N(K_2), s)$. So if it is surjective then the map

$$\mathrm{HF}^n(S^3_N(K_2), s) \to \mathrm{HF}^n(S^3)$$

is also surjective. So we get that $\nu_n(K_1) \geq \nu_n(K_2)$. The same argument with K_1 and K_2 switched shows the inequality $\nu_n(K_2) \geq \nu_n(K_1)$. Therefore $\nu_n(K_1) = \nu_n(K_2)$.

For negative n, that $\nu_n(K)$ is a concordance invariant follows from a similar argument to the above. □

Lemma 5.2.4 (Large Negative Integer Surgery Formula for HF^n)**.** *Consider the subquotient complex*

$$\mathrm{CFK}^n(S^3, K, m) = \mathrm{CFK}^\infty(S^3, K)\{0 \leq \min(i, j - m) \leq n - 1\}$$

of $\mathrm{CFK}^+(S^3,K,m)$ *generated by* $[\boldsymbol{x},i,j]$ *with* $0\le \min(i,j-m)\le n-1$. *The map* Φ *of Ozsvath-Szabo induces isomorphisms in the following diagram:*

$$\begin{array}{ccccccccc} 0 & \longrightarrow & \mathrm{CFK}^n(Y,K,m) & \longrightarrow & \mathrm{CFK}^+(Y,K,m) & \xrightarrow{U^n} & \mathrm{CFK}^+(Y,K,m) & \longrightarrow & 0 \\ & & \downarrow{\scriptstyle \Phi(n)} & & \downarrow{\scriptstyle \Phi^+} & & \downarrow{\scriptstyle \Phi^+} & & \\ 0 & \longrightarrow & \mathrm{CF}^n(Y_{-p}K,[m]) & \longrightarrow & \mathrm{CF}^+(Y_{-p}K,[m]) & \xrightarrow{U^n} & \mathrm{CF}^+(Y_{-p}K,[m]) & \longrightarrow & 0. \end{array}$$

Proof. The map Φ^+ is an isomorphism of chain complexes by Theorem 4.1 of [23]. By the Five Lemma, so is $\Phi(n)$. □

Lemma 5.2.5 (Large Positive Integer Surgery Formula for HF^n)**.** *The subquotient complex*

$$\mathrm{CFK}^n(S^3,K,m)=\mathrm{CFK}^\infty(S^3,K)\{0\le \max(i,j-m)\le n-1\},$$

of $\mathrm{CFK}^+(Y,K,m)$ *generated by* $[\boldsymbol{x},i,j]$ *with* $0\le \max(i,j-s)\le n-1$, *is isomorphic to* $\mathrm{CF}^n(S^3_N(K),m)$ *as chain complexes.*

The map Ψ *of Ozsvath-Szabo induces isomorphisms in the following diagram:*

$$\begin{array}{ccccccccc} 0 & \longrightarrow & \mathrm{CF}^n(Y_pK,[m]) & \longrightarrow & \mathrm{CFK}^+(Y_pK,[m]) & \xrightarrow{U^n} & \mathrm{CFK}^+(Y_pK,[m]) & \longrightarrow & 0 \\ & & \downarrow{\scriptstyle \Psi(n)} & & \downarrow{\scriptstyle \Psi^+} & & \downarrow{\scriptstyle \Psi^+} & & \\ 0 & \longrightarrow & \mathrm{CFK}^n(Y,K,m) & \longrightarrow & {}^b\,\mathrm{CFK}^+(Y,K,m) & \xrightarrow{U^n} & {}^b\,\mathrm{CFK}^+(Y,K,m) & \longrightarrow & 0. \end{array}$$

Proof. The map Ψ^+ is an isomorphism of chain complexes by Theorem 4.4 of [23]. By the Five Lemma, so is $\Psi(n)$. □

Proposition 5.2.6. Monotonicity: $\nu_n(K)\le \nu_{n+1}(K)$.

Proof. For positive n, consider the commutative diagram

$$\begin{array}{ccc} \mathrm{HF}^{n+1}(S^3_NK,s) & \xrightarrow{v_{n+1,s}} & \mathrm{HF}^{n+1}(S^3) \\ \downarrow{\scriptstyle \cdot U} & & \downarrow{\scriptstyle \cdot U} \\ \mathrm{HF}^{n}(S^3_NK,s) & \xrightarrow{v_{n,s}} & \mathrm{HF}^{n}(S^3) \end{array}$$

where the vertical maps are given by multiplication by U. The vertical map on the right is surjective. Thus, if $v_{n+1,s}$ is surjective, then so is $v_{n,s}$.

For negative n, consider the commutative diagram

$$\begin{array}{ccc} \mathrm{HF}^{-n}(S^3) & \xrightarrow{v'_{-n,s}} & \mathrm{HF}^{-n}(S^3_{-N}K,s) \\ \downarrow{\scriptstyle i'_a} & & \downarrow{\scriptstyle i'_b} \\ \mathrm{HF}^{-(n-1)}(S^3) & \xrightarrow{v'_{-(n-1),s}} & \mathrm{HF}^{-(n-1)}(S^3_{-N}K,s) \end{array}$$

where the vertical maps are induced by inclusion of chain groups. In particular, the left map i'_a is injective on homology. Therefore, if $v_{-(n-1),s}(K)$ is injective, then so is $v_{-n,s}(K)$. We conclude that $\nu_{n-1}(K) \leq \nu_n(K)$. □

Proposition 5.2.7. Stabilization: *For sufficiently large positive n, $\nu_n = \nu^+(K)$. For sufficiently large negative n, $\nu_n = \nu^{+'}(K)$.*

Proof. For sufficiently large n, we show that if the map $v_s^+ : \mathrm{HF}^+(S^3_N K,s) \to \mathrm{HF}^+(S^3)$ restricted to $\mathfrak{T}^+$ has nontrivial kernel, then the map $v_{n,s} : \mathrm{HF}^n(S^3_N K,s) \to \mathrm{HF}^n(S^3)$ cannot be surjective on homology.

There is a canonical degree shifting isomorphism

$$\mathrm{CF}^n(Y) \cong \mathrm{CF}^-(Y) \otimes_{\mathbb{F}[U]} \frac{\mathbb{F}[U]}{U^n}.$$

Let $C_1 = \mathrm{CF}^-(S^3_N K,s)$ and $C_2 = \mathrm{CF}^-(S^3)$. By the universal coefficient theorem:

$$\begin{array}{ccccccc} 0 \to H_*(C_1) \otimes \frac{\mathbb{F}[U]}{U^n} & \xrightarrow{i_1} & H_*(C_1 \otimes \frac{\mathbb{F}[U]}{U^n}) & \longrightarrow & \mathrm{Tor}(H_*C_1, \frac{\mathbb{F}[U]}{U^n}) \to 0 \\ \downarrow{\scriptstyle v_s^- \otimes} & & \downarrow{\scriptstyle v^-_{n,s}} & & \downarrow{\scriptstyle \mathrm{Tor}(v_s^-)} \\ 0 \to H_*(C_2) \otimes \frac{\mathbb{F}[U]}{U^n} & \xrightarrow{i_2} & H_*(C_2 \otimes \frac{\mathbb{F}[U]}{U^n}) & \longrightarrow & \mathrm{Tor}(H_*C_2, \frac{\mathbb{F}[U]}{U^n}) \to 0 \end{array}$$

where all tensor products are taken over $\mathbb{F}[U]$. The middle vertical map $v^-_{n,s}$ is the same as the map $v_{n,s} : \mathrm{HF}^n(S^3_N K,s) \to \mathrm{HF}^n(S^3)$.

Note that $\mathrm{HF}^-(Y)/\{U\text{-torsion}\} = \mathfrak{T}^- = \mathbb{F}[U]$ for Y a rational homology 3-sphere. So $H_*(C_1) = \mathfrak{T}^- \bigoplus (\oplus \frac{\mathbb{F}[U]}{U^{m_i}})$.

Assume n is sufficiently large so that $m_i < n$ for all m_i. Note that $\mathrm{Tor}(\frac{\mathbb{F}[U]}{U^m}, \frac{\mathbb{F}[U]}{U^n}) = \frac{\mathbb{F}[U]}{U^m}$ if $m < n$, so the above Tor groups are $n-1$ torsion. In addition, $\mathfrak{T}^- \otimes \frac{\mathbb{F}[U]}{U^n} = \frac{\mathbb{F}[U]}{U^n}$ and $\frac{\mathbb{F}[U]}{U^{m_i}} \otimes \frac{\mathbb{F}[U]}{U^n} = \frac{\mathbb{F}[U]}{U^{m_i}}$.

If $v_s^+|_{\mathfrak{T}^+}$ has nontrivial kernel, then v_s^- is not surjective. So for sufficiently large n, the image of $v_s^- \otimes$ is $n-1$ $U-$torsion. Therefore, the image of $v^-_{n,s} \circ i_1$ is $n-1$ $U-$torsion.

Suppose $\xi \in H_*(C_1 \otimes \frac{\mathbb{F}[U]}{U^n})$ such that $v^-_{n,s}(\xi)$ is an element of order n. Then since the short exact sequence in the universal coefficient theorem splits, $\xi = \alpha + \beta$ where $\alpha \in H_*(C_1) \otimes \frac{\mathbb{F}[U]}{U^n}$ and $\beta \in \mathrm{Tor}(H_*C_1, \frac{\mathbb{F}[U]}{U^n})$. But

$$U^{n-1} \cdot v^-_{n,s}(\alpha + \beta) = v^-_{n,s}(U^{n-1}\alpha) + v^-_{n,s}(U^{n-1}\beta) = 0.$$

Since $H_*(C_2 \otimes \frac{\mathbb{F}[U]}{U^n}) = \frac{\mathbb{F}[U]}{U^n}$, $v^-_{n,s}$ is not surjective. Therefore, for sufficiently large n, $\nu_n = \nu^+$.

□

Example 5.2.8. In Figure 5.1 we give an example of a one-parameter family of $\mathbb{Z}\oplus\mathbb{Z}$-filtered chain complexes such that $\nu^+ = 0$ and $\nu^{+'} = -h$ for a fixed constant h. For negative n, the sequence ν_n distinguishes these chain complexes by detecting the length l of the diagonal arrow.

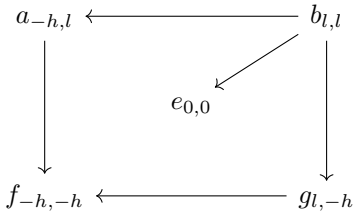


Figure 5.1

The subscripts (i, j) denote the the i-filtration and the Alexander filtration j of the generator.

For $n = -1, \ldots, -l$, $\nu_n = 0$. For $n \leq -l - 1$, $\nu_n = -h$.

Note that this example is purely algebraic and it is not known whether this complex is the knot Floer chain complex of a knot.

Example 5.2.9. The (3,4) torus knot $T_{3,4}$ has $\tau = -3$, $\nu = -2$, and $\nu^+ = 0$. The sequence ν_n jumps from $\nu_1 = \nu = -2$ directly to $\nu_2 = \nu^+ = 0$.

Example 5.2.9 shows that the sequence ν_n can increase by more than one at a time, in contrast to the local h-invariants defined by Rasmussen, which jump by at most one (Proposition 7.6, [31]).

Example 5.2.10. There may exist several jumps in the sequence ν_n as it ranges from ν to ν^+. Figure 5.3(a) shows the knot Floer chain complex CFK^∞ of the $(2, 9)$-torus knot. The sequence ν_n starts at $\nu_{-1} = \nu' = 3$, $\nu_{-2} = 1$, $\nu_{-3} = 0 = \nu^{+'}$. See Figure 5.3 for details. As evident, there is an intermediate value of ν_n in between ν' and $\nu^{+'}$.

More generally, the $(2, 2n + 1)$-torus knot $T_{2,2n+1}$ has $\tau = n$, $\nu' = n - 1$, and $\nu^{+'} = 0$. The sequence ν_n starts at ν' and decreases by two until it reaches 1 or 0, at which point it stabilizes to zero.

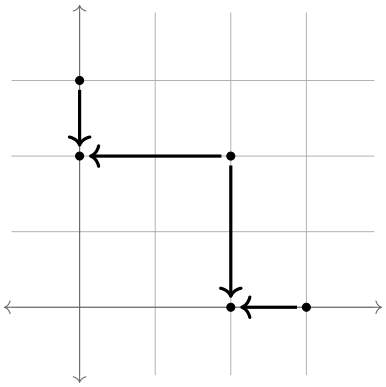
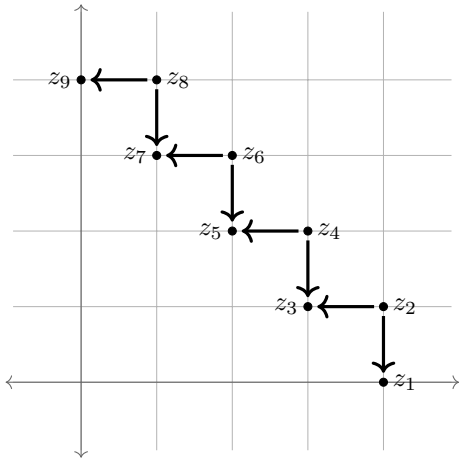
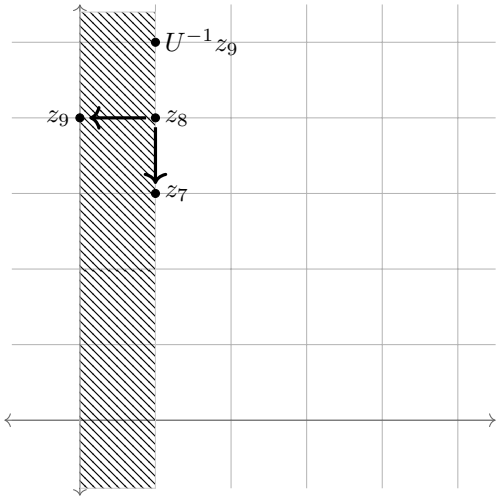


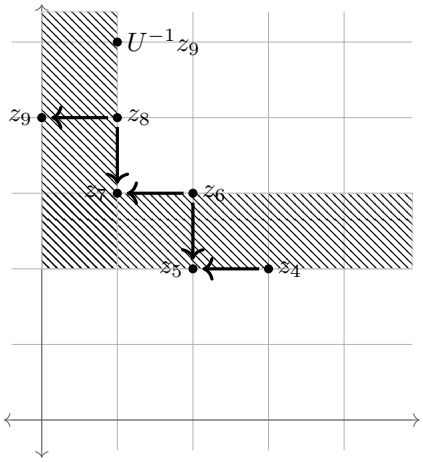
Figure 5.2: Generating complex for CFK^∞ of the left-handed (3,4)-torus knot $T_{3,4}$
$\mathrm{CFK}^\infty(T_{3,4})$ is generated over $\mathbb{F}[U, U^{-1}]$ by the above chain complex. The arrows are drawn to scale and have length one or two. This diagram is taken from Figure 11.5 in [16].



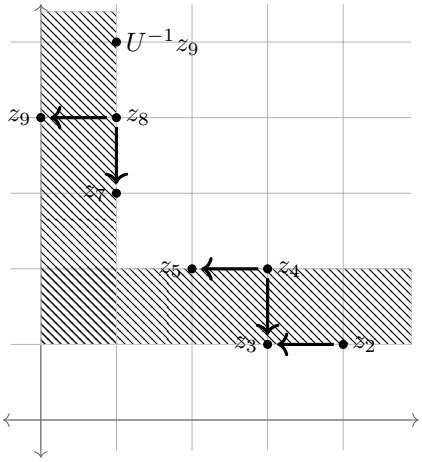
(a) Generating complex for CFK^∞ of the (2, 9)-torus knot $T_{2,9}$



(b) Generators $U^{-1}z_9$ and $z_9 + z_7$ for $\mathrm{HF}^2(S^3)$



(c) The generators $\{z_i\}$ in $\mathrm{HF}^2(S^3_{-N}K, [2])$ vanish in homology



(d) The generators $\{z_9 + z_7\}$ and $U^{-1}z_9$ in $\mathrm{HF}^2(S^3_{-N}K, [1])$ survive

Figure 5.3

Bibliography

[1] József Bodnár, Daniele Celoria, and Marco Golla, *Cuspidal curves and Heegaard Floer homology*, Proc. Lond. Math. Soc. (3) **112** (2016), no. 3, 512–548. MR 3474482

[2] Vincent Colin, Paolo Ghiggini, and Ko Honda, *Equivalence of Heegaard Floer homology and embedded contact homology via open book decompositions*, Proc. Natl. Acad. Sci. USA **108** (2011), no. 20, 8100–8105. MR 2806645 (2012f:53190)

[3] Hisaaki Endo, *Linear independence of topologically slice knots in the smooth cobordism group*, Topology Appl. **63** (1995), no. 3, 257–262. MR 1334309

[4] Robert E. Gompf and András I. Stipsicz, 4-*manifolds and Kirby calculus*, Graduate Studies in Mathematics, vol. 20, American Mathematical Society, Providence, RI, 1999. MR 1707327

[5] Matthew Hedden, *Knot Floer homology of Whitehead doubles*, Geom. Topol. **11** (2007), 2277–2338. MR 2372849 (2008m:57030)

[6] Jennifer Hom, *Bordered Heegaard Floer homology and the tau-invariant of cable knots*, J. Topol. **7** (2014), no. 2, 287–326. MR 3217622

[7] ———, *The knot Floer complex and the smooth concordance group*, Comment. Math. Helv. **89** (2014), no. 3, 537–570. MR 3260841

[8] ———, *A survey on Heegaard Floer homology and concordance*, arXiv:1512.00383 (2015).

[9] ———, *An infinite-rank summand of topologically slice knots*, Geom. Topol. **19** (2015), no. 2, 1063–1110. MR 3336278

[10] ———, *A note on the concordance invariants epsilon and upsilon*, Proc. Amer. Math. Soc. **144** (2016), no. 2, 897–902. MR 3430863

[11] Jennifer Hom and Zhongtao Wu, *Four-ball genus bounds and a refinement of the Ozsvath-Szabo tau-invariant*, arXiv:1401.1565 (2014).

[12] Stanislav Jabuka, *Concordance invariants from higher order covers*, Topology Appl. **159** (2012), no. 10-11, 2694–2710. MR 2923439

[13] Peter Kronheimer and Tomasz Mrowka, *Gauge theory for embedded surfaces. II*, Topology **34** (1995), no. 1, 37–97. MR 1308489 (96b:57038)

[14] Çağatay Kutluhan, Yi-Jen Lee, and Clifford H. Taubes, *HF=HM I : Heegaard Floer homology and Seiberg–Witten Floer homology*, arXiv:1007.1979 (2010).

[15] Adam Simon Levine, *Slicing mixed Bing-Whitehead doubles*, J. Topol. **5** (2012), no. 3, 713–726. MR 2971611

[16] Robert Lipshitz, Peter Ozsváth, and Dylan Thurston, *Bordered Heegaard Floer homology: Invariance and pairing*, arXiv:0810.0687 (2008).

[17] ———, *Notes on bordered Floer homology*, Contact and symplectic topology, Bolyai Soc. Math. Stud., vol. 26, János Bolyai Math. Soc., Budapest, 2014, pp. 275–355. MR 3220945

[18] Charles Livingston, *Slice knots with distinct Ozsváth-Szabó and Rasmussen invariants*, Proc. Amer. Math. Soc. **136** (2008), no. 1, 347–349 (electronic). MR 2350422

[19] Ciprian Manolescu and Brendan Owens, *A concordance invariant from the Floer homology of double branched covers*, Int. Math. Res. Not. IMRN (2007), no. 20, Art. ID rnm077, 21. MR 2363303

[20] Ciprian Manolescu and Peter Ozsváth, *Heegaard Floer homology and integer surgeries on links*, arXiv:1011.1317 (2010).

[21] Peter Ozsváth, András Stipsicz, and Zoltán Szabó, *Concordance homomorphisms from knot Floer homology*, arXiv:1407.1795 (2014).

[22] Peter Ozsváth and Zoltán Szabó, *Knot Floer homology and the four-ball genus*, Geom. Topol. **7** (2003), 615–639. MR 2026543 (2004i:57036)

[23] ———, *Holomorphic disks and knot invariants*, Adv. Math. **186** (2004), no. 1, 58–116. MR 2065507 (2005e:57044)

[24] ———, *Holomorphic disks and three-manifold invariants: properties and applications*, Ann. of Math. (2) **159** (2004), no. 3, 1159–1245. MR 2113020 (2006b:57017)

[25] ———, *Holomorphic disks and topological invariants for closed three-manifolds*, Ann. of Math. (2) **159** (2004), no. 3, 1027–1158. MR 2113019 (2006b:57016)

[26] ———, *Holomorphic triangles and invariants for smooth four-manifolds*, Adv. Math. **202** (2006), no. 2, 326–400. MR 2222356 (2007i:57029)

[27] ———, *Knot Floer homology and integer surgeries*, Algebr. Geom. Topol. **8** (2008), no. 1, 101–153. MR 2377279

[28] ———, *Knot Floer homology and rational surgeries*, Algebr. Geom. Topol. **11** (2011), no. 1, 1–68. MR 2764036

[29] Thomas D. Peters, *A concordance invariant from the Floer homology of +/- 1 surgeries*, arXiv:1003.3038 (2010).

[30] Ina Petkova, *Cables of thin knots and bordered Heegaard Floer homology*, Quantum Topol. **4** (2013), no. 4, 377–409. MR 3134023

[31] Jacob Rasmussen, *Floer homology and knot complements*, ProQuest LLC, Ann Arbor, MI, 2003, Thesis (Ph.D.)–Harvard University. MR 2704683

[32] ———, *Khovanov homology and the slice genus*, Invent. Math. **182** (2010), no. 2, 419–447. MR 2729272 (2011k:57020)

[33] Vladimir Turaev, *Torsion invariants of* Spin^c*-structures on* 3*-manifolds*, Math. Res. Lett. **4** (1997), no. 5, 679–695. MR 1484699